SHORT TIME-SCALE AND SEASONAL VARIABILITY OF POREWATER CONSTITUENTS IN A PERMEABLE NEARSHORE SEDIMENT

A THESIS SUBMITTED TO THE GRADUATE DIVISION OF THE UNIVERSITY OF HAWAI‘I IN PARTIAL FULFILLMENT OF THE REQUIREMENTS FOR THE DEGREE OF

MASTER OF SCIENCE

IN

OCEANOGRAPHY

DECEMBER 2010

By
Kristen Fogaren

Thesis Committee:

Francis J. Sansone, Chairperson
Eric H. De Carlo
Margaret A. McManus

We certify that we have read this thesis and that, in our opinion, it is satisfactory in scope and quality as a thesis for the Degree of Master in Science in Oceanography.

THESIS COMMITTEE

_____
Chairperson

_____

_____

Acknowledgements

I would like to thank the members of my Thesis Committee, Frank Sansone, Eric De Carlo and Margaret McManus, for their wonderful guidance, mentorship and patience throughout my time here at the University of Hawai‘i. I would also like to thank the many people who made this possible: Chris Colgrove, Jon Fram, Kevin Stierhoff and Kimball Millikan for their invaluable assistance in the field; Rebecca Briggs, Chip Young and the rest of the Ruttenberg lab for their support and the use of their space and equipment; and my mom, dad, sister and brother for their unconditional support in everything I pursue. The following people have supported me during my journey here in the Oceanography Department, and I am forever indebted to them: M. Iacchei, J. Puritz, J. Stopa, K. MacDonald, B. Baltes, R. Simpson, K. Nolan, C. Bradley, T. Campbell, A. Fetherolf, J. Sevadjian, J. Wells, J. Murphy, I. Chen, A. Hannides, M. Tomlinson, L. Oswald, M. Grand, A. Choy, A. Richie, C. Coleman, P. Bienfang, K. Ruttenburg, C. Measures, K. Lopes, P. Drupp, D. Smith, M. Atkinson and C. Glenn. I would like to acknowledge the National Science Foundation for funding this research. Also, I would like to thank the Oceanography Department, Geno Pawlak, Eric De Carlo, Frank Sansone, Steve Dollar and Brian Glazer for providing graduate support during my journey. Lastly, a special thanks to Kathy Kozuma for always going above and beyond.

Abstract

Porewater samples were collected from a nearshore permeable sediment at the Kilo Nalu Nearshore Observatory, O‘ahu, Hawai‘i over a variety of surface gravity wave conditions to evaluate the effect of ocean swells and their corresponding bottom currents on dissolved oxygen and nutrient dynamics in porewater. Our results indicate that swell events, resulting in nearbed velocities greater than 0.30 m/s, affect porewater constituents to a depth of ~7.5 cm by causing enhanced flushing between the porewater in the uppermost sediment and the overlying water column. This process is associated with a fluorescence response in the bottom water, suggesting that the flushing and subsequent nutrient input to the water column may be important to nutrient budgets in nearshore oligotrophic waters. Increased nearbed velocities were correlated with greater depth-integrated dissolved oxygen concentrations, suggesting that a larger amount of dissolved oxygen is injected in the sediment with larger significant wave heights and their correspondingly larger nearbed velocities. Seasonal variability in the physical environment appears to be linked to available amounts of total nitrate + nitrite in the sediment, with greater amounts available during the summer months, when the sediments are more aerated due to more intense austral winter wave action on the south shore of O‘ahu. Ratios of regenerated nutrients suggest that the majority of the organic matter undergoing remineralization is planktonic in origin. However, a shift in source matter undergoing remineralization coincided with a late-summer swell event, suggesting that swell events and/or seasonality may be important factors in controlling the organic matter supplied to the sediments at Kilo Nalu Nearshore Observatory.

Table of Contents

Acknowledgements iii
Abstract iv
1. Introduction 1
2. Study Area 3
    2.1 Swell Conditions 4
    2.2 Ala Wai Canal Watershed 5
3. Methods 5
    3.1 Measurement of Wave and Water-Column Characteristics 5
    3.2 Sampling and Analysis of Sediment 6
    3.3 Sampling and Analysis of Porewater 7
    3.4 Data Corrections 10
    3.5 Depth Integrations of Porewater Concentrations 12
4. Results 12
    4.1 Sediment and Porewater Characterization 12
    4.2 July-August 2008 Swell: Small Surface Gravity Wave Event 13
    4.3 September 2008 Swell: Larger Surface Gravity Wave Event 14
    4.4 December 2008 Swell: Large Kona Swell Event 16
5. Discussion 18
    5.1 Nutrient-nutrient Relationships 18
        5.1.1 C:P Relationship 19
        5.1.2 C:Si Relationship 19
    5.2 Depth-Integrated Porewater Concentrations 20
        5.2.1 Depth-Integrated $Si(OH)_4$ Concentrations 20
        5.2.2 Depth-Integrated DO and NO_x Concentrations 21
    5.3 Porewater flushing and biological response to swell events 23
6. Conclusions 24
7. References 25

Table of Figures

Figure 1: Map of Māmala Bay and southern Oʻahu 31
Figure 2: Map of Kilo Nalu Nearshore Observatory 32
Figure 3: Biofouled and corrected fluorescence data 33
Figure 4: Porewater DIC concentrations.....34
Figure 5: Significant wave heights and nearbed velocities, July-August 2008 Event.....35
Figure 6: Porewater nutrient concentrations, July-August 2008 Event 36
Figure 7: Water-column turbidity and fluorescence levels, July-August 2008 Event.....37
Figure 8: Significant wave heights and nearbed velocities, September 2008 Event 38
Figure 9: Porewater nutrient and DO concentrations, September 2008 Event 39
Figure 10: Water-column turbidity and fluorescence levels, September 2008 Event 40
Figure 11: Significant wave heights and nearbed velocities, December 2008 Event.....41
Figure 12: Rainfall, salinity and temperature at Kilo Nalu, December 2008 Event.....42
Figure 13: WQB-AW and WQB-KN salinity, December 2008 Event.....43
Figure 14: WQB-AW and WQB-KN turbidity levels, December 2008 Event.....44
Figure 15: Water-column turbidity and fluorescence levels, December 2008 Event.....45
Figure 16: Porewater nutrient, DO and DIC concentrations, December 2008 Event.....46
Figure 17: Respired PO_4 and respired $Si(OH)_4$ versus respired DIC 47
Figure 18: Depth-integrated $Si(OH)_4$, PO_4 and NO_x porewater concentrations.....48
Figure 19: Porewater $Si(OH)_4$ concentrations versus PO_4 concentrations 49
Figure 20: Depth-integrated NO_x and DO concentrations versus nearbed velocities.....50
Figure 21: Turbidity and fluorescence levels during July, Sept. and Dec 2008 Events 51

Table of Appendices

Appendix A: Porewater Data 52
Appendix B: Oxygen Contamination Experiment 61
Appendix C: Porewater Nitrate: Reductase Enzyme vs. Cadmium Reduction 62
Appendix D: Wave and Tidal Data 64
Appendix E: Bottom Water Salinity, Temperature, Fluorescence and Turbidity Data 72

1. Introduction

Despite the fact that sandy, highly permeable sediments cover ~44% of the world's continental shelves (Riedl et al., 1972), the role of these sediments in coastal biogeochemical cycles has historically been neglected (Boudreau et al., 2001). Permeable sediments have been ignored for two reasons. First, the conventional methods of sampling in fine-grained environments (e.g., coring, benthic chambers) either do not work, or alter fundamental sandy sediment dynamics, making sampling in these areas more difficult (Boudreau et al., 2001; Jahnke, 2004).

Additionally, permeable sediments typically have lower organic matter content compared to their fine-grained counterparts (Meyer-Reil, 1986; Boudreau et al., 2001), resulting in the misperception that permeable sediments were relatively biogeochemically inactive (Boudreau et al., 2001; Rocha, 2008). It was not until organic-poor sands were found to have high oxygen consumption rates (Reimers et al., 2004), that this misperception of permeable sediments began to change. In fact, high oxygen consumption rates coupled with lower organic matter content suggests that permeable sediment have the ability to be sites of high biogeochemical activity and the potential for efficient organic matter remineralization (Huettel et al., 1998; Rocha, 2008). Thus, permeable sediments have the ability to support high metabolic rates, even matching those found in organic-rich, fine grained sediments (Jahnke et al., 2000; Jahnke et al., 2005).

It has been traditionally thought that, as organic matter undergoes remineralization in the sediments, inorganic nutrients are regenerated and the release of inorganic nutrients results in enhanced water column productivity (Rowe, 1975; Marinelli et al., 1998; Jahnke, 2004). This remineralization process applies to both fine-grained and permeable sediments. Permeable sediments have the potential to support higher metabolic rates and nutrient cycling despite lower amounts of organic matter (e.g., Webb and Theodor, 1968) because permeable sediments often

subject to advective processes (e.g., bottom currents, surface gravity waves; Shum and Sundby, 1996).

Permeable sediments can support high metabolic rates through enhanced fluid transport between the water column and porewater in three ways. First, enhanced porewater flow results as bottom currents flow over small topographic features such as sediment ripples, infauna mounds and benthic fauna, with the flow over topographic features creating pressure gradients that drive fluid exchange between the sediment and the water column after Bernoulli's principle (Huettel and Gust, 1992; Huettel et al., 1996; Boudreau et al., 2001). In the case of rippled sediment, fluid from the water column enters the sediment ripples through areas of high pressure found at the troughs, and exits through areas of low pressure found at the crests (Shum and Sundby, 1996).

Second, surface gravity waves are important mechanisms leading to enhanced transport in permeable sediments found in wave-impacted environments (e.g., Falter and Sansone, 2000b). As surface gravity waves pass over a permeable sediment, they cause a dynamic pressure field that produces bottom currents (Shum and Sundby, 1996; Huettel et al., 1996). Despite the temporal variability of these wave events, surface gravity waves have been shown to be important in regulating porewater chemistry by controlling porewater movement and chemical zonation in carbonate sands (Boudreau et al., 2001).

Last, enhanced porewater flow can force degradable particles like bacteria, algae, diatoms and detritus into the sediment where they can be retained (Huettel et al., 1996; Huettel and Rusch, 2000). This filtration of particles increases the transfer rate of particulate matter across the sediment-water interface. Also, enhanced porewater flow can result in particle penetration deeper into the sediment than what typically occur through simple gravitational settling (Huettel et al., 1996). For example, Rusch and Huettel (2000) demonstrated that bottom currents can physically

force diatoms ~2.2 cm into a permeable sediment. Oxygen and other electron acceptors that are flushed into the sediments through the principles discussed previously enhance particle decay, resulting in the high metabolic rates found in permeable rates (Boudreau et al., 2001).

With an increased supply of organic matter and electron acceptors to support rapid remineralization, remineralized constituents can be released into the overlying water column at enhanced rates (Huettel et al., 1998). In oligotrophic waters, inorganic nutrients produced in remineralization may be an important source of nutrients to the water column. For example, in a year-long comparison study of coral reefs on the southern shore of O‘ahu, Hawai‘i, water-column concentrations of dissolved nitrate and ammonium were seen to increase during three ocean swell events (Grigg, 1995).

Therefore, the connection between sediment organic matter remineralization, inorganic nutrient production and water-column productivity may be important in coastal biogeochemical systems with permeable sediments. Here we report on porewater inorganic nutrient and dissolved oxygen dynamics in a nearshore permeable sediment. Samples were collected over a variety of surface gravity wave conditions in order to evaluate the effect of ocean swell events on porewater and water-column nutrient concentrations. Our results suggest that swell events (resulting in nearbed velocities > 0.30 m/s) affect porewater inorganic nutrients and dissolved oxygen to a depth of ~7.5 cm by flushing the sediment, and that this process is associated with a fluorescence response in the bottom water.

2. Study Area

Our study site was located at the Kilo Nalu Nearshore Reef Observatory in Māmala Bay on the south shore of O‘ahu, Hawai‘i (Figure 1) (Sansone et al., 2008). The infrastructure deployed at Kilo Nalu allows *in situ* physical data to be accessed in near real-time via data and

power connections to a shore-based station. Near-real time data from the observatory are available at www.soest.hawaii.edu/OE/KiloNalu/.

2.1 Swell Conditions

The south shore of O‘ahu, the site of the Kilo Nalu Observatory, can be characterized as having four types of ocean swell events (Fletcher et al., 2002). The first and most common is Trade Wind Swell originating from the northeast (~45°) and wrapping around the southern flank of Diamond Head (Figure 1). These events persist most of the year and have typical wave heights of 0.3 to 1.3 m, with periods of 5-8 s (Fletcher et al., 2002). The second type of event is Southern Swell that is generated in the southern hemisphere by austral winter storms. These occur mostly in summer and early autumn from April to October; they are usually from the south (~180°) but can originate anywhere from 147° to 210° (Fletcher et al., 2002). Southern swells typically result in waves ranging from 0.3 to 1.2 m in height with 14- to 22-s periods, but can result in waves as high as 5.5 m with 25-s periods in fully developed seas (Moberly and Chamberlain, 1964; Fletcher et al., 2002). The third type of swell event observed on the south shore is swell associated with the Kona Storm. These localized storms are generated by atmospheric low pressure systems, with ocean waves developing from southerly to southwesterly winds (Moberly and Chamberlain, 1964). These storms can occur at any time of the year but typically occur in winter, resulting in 0.9- to 1.5-m waves with 8- to10-s periods (Fletcher et al., 2002); however, waves reaching heights of 5 m have been observed under extreme circumstances (Moberly and Chamberlain, 1964). The fourth and least frequent type of swell that impacts the south shore is hurricane related swell (Fletcher et al., 2002).

2.2 Ala Wai Canal Watershed

The Ala Wai Canal is a manmade estuary completed in the 1920's that drains the Ala Wai Watershed into Māmala Bay (Fryer, 1995). The 41.6 km^2 watershed consists of ~46% forested conservation land, mostly found at high elevations, with the remaining watershed at lower elevations classified as urban (Fryer, 1995). The Mānoa and Pālolo streams are the two major tributaries and are responsible for ~58% of the water flow into the Ala Wai Canal (Fryer, 1995). National Weather Service (NWS) rain gauges collect rainfall data in 15-min intervals at the Mānoa-Lyon Arboretum in Mānoa Valley (MLA) and in downtown Honolulu at Aloha Towers (ALO) (Figure 1). A United States Geological Survey (USGS) stream gauge located on the Mānoa-Pālolo Drainage Canal (USGS 16247100) a few hundred meters above the Ala Wai Canal provided stream flow rates.

3. Methods

3.1 Measurement of Wave and Water-Column Characteristics

The instruments utilized in this study were deployed at the Kilo Nalu Nearshore Observatory in 12 m of water (Figure 2), approximately 400 m from shore. They included a 1200-kHz acoustic Doppler current profiler (ADCP; RDI-Teledyne, Poway, CA, USA), a Seabird-37 conductivity-temperature-depth (CTD) recorder (Sea-Bird Electronics, Inc., Bellevue, WA, USA) and an ECO FLNTU sensor (WET Labs, Philomath, OR, USA). The ADCP measured near-bed current velocity, surface wave characteristics and tidal levels. The CTD measured conductivity, temperature and pressure, enabling the physical water properties (salinity, temperature, density and depth) to be obtained. The ECO FLNTU sensor measured turbidity and fluorescence as a proxy for particle matter loading and biological productivity, respectively (Sansone et al., 2008).

A 1200-kHz RDI-Teledyne ADCP was deployed continuously at Kilo Nalu. This bottom-mounted, upward-looking instrument was configured to collect high-resolution ensemble pressure and velocity data at 1 Hz. Velocity readings were collected starting at 0.45 m above the SWI, continuing upward throughout the water column at a vertical resolution of 25 cm. Current velocities were averaged every 20 min, and wave data presented in this study were calculated over 20-min periods. Twenty-min averaging period represents the shortest period of time over which we can reasonably calculate wave statistics. In this study, significant wave height (H_{sig}) was determined by the spectral method (Emery and Thomson, 2004), where H_{sig} is equal to 4 times the integral under the power spectrum (wave energy as a function of frequency). This is equivalent to the mean of the one-third largest waves. Nearbed velocities (V_{bed}) was a measure of wave induced velocity and was defined as the mean of the highest one-third of the velocity readings recorded in the bottom 3 m.

Additionally, two surface water quality buoys (WQBs) were equipped with Seabird-16*plus* V2 SEACAT C-T recorders and ECO FLNTU sensors to provide conductivity, temperature, fluorescence and turbidity measurements ~1 m from the surface. As a part of the Hawaii Ocean Observing System (HiOOS) described by Tomlinson et al. (in prep. 2010), the first buoy was located 335 m from the mouth of the Ala Wai Canal (WQB-AW) and the second water quality buoy was located at Kilo Nalu Observatory (WQB-KN), situated ~2 km west of the Ala Wai Canal mouth (Figure1).

3.2 Sampling and Analysis of Sediment

The sediment at Kilo Nalu consists of coral, limestone and other carbonate material (Sansone et al., 2008). A grab sediment sample was manually collected by divers to characterize the top ~10 cm of sediment near the porewater wells (described in Section 3.3). An

estimate of sediment organic content was determined in triplicate by loss-on-ignition, measured by combusting the sediment for 4.5 hours at 550 °C. Grain size analysis was then performed in triplicate on this post-combusted sediment by mixing ~200-g samples and dry sieving them through seven sieves (2 mm, 1 mm, 500 µm, 250 µm, 125 µm, 63 µm, and 30µm mesh size).

3.3 Sampling and Analysis of Porewater

To obtain sediment porewater samples at Kilo Nalu, six wells, each 1 m in length, were constructed using 1.25-cm diameter schedule 80 PVC pipe and PVC ball valves (Falter and Sansone, 2000a, Falter and Sansone, 2000b). Each well had a sampling port at a specified depth, and a ~3-cm length of epoxy resin was used to plug the PVC pipe below the sampling port. The remaining empty space below the plug was filled with sand to guarantee that the well was negatively buoyant In addition, wells were externally grooved every 5 cm to hinder water movement along the outside of the well during sampling and to restrict the upward movement of the well itself. Porewater wells with collection depths at 7.5, 15, 20, 30, 40 and 50 cm below the sediment-water interface (SWI) were manually installed in the sand patch at the Kilo Nalu 12-m site by divers using a chisel-tipped stainless steel rod and a fence-post driver. First, the fence-post driver was used to drive the rod into the sediment. Then, the rod was removed from the sediment and a porewater well was quickly inserted in its place. The rod created a vacant space about 4 cm in diameter and 1 m in length, which ensured that no damage occurred to the wells during installation. The first sampling did not occur until two weeks after installation to allow the sampling environment time to return to background conditions.

The wells were deployed in a rectangular 20 x 10 cm area. The specific arrangement of the wells ensured close proximity to adjacent wells, while minimizing interference between wells (Falter and Sansone, 2000a). Using a porosity of 0.49 and a porewater sample volume of

140 mL, the sampling volume in the sediment was estimated to be ~4 cm in radius. A porosity of 0.49 is representative of sandy sediment at Kilo Nalu (Hebert et al., 2007).

Discrete porewater samples were collected on 29 separate occasions over a variety of physical conditions in a ~29 month period beginning on 26 August 2007 and ending on 29 January 2010. Time spans between sampling dates varied from 2 days to 6 months. Intensive sampling occurred during June-December 2008, with 18 sampling dates within that 6-month period. During a large swell event in late summer 2008, the wells were partially scoured out of the sediment and were no longer at their intended depths. As a result, the original porewater array, which was installed in early 2006, was removed and replaced with a new array on 7 October 2008.

A sample from each well, as well as from the SWI, was collected manually by divers on each sampling date using 140-mL Monoject plastic syringes (Covidien, Mansfield, MA, USA), for a total of 7 samples for each sampling day. The SWI sample was collected 2-3 mm above the SWI by holding Tygon tubing, connected to the syringe by a two-way stop cock, flush with the sediment surface. Porewater sample collection from each well began after the dead volume in the well was removed in order to guarantee sampling from the desired sediment depth. The dead volume was removed by drawing and discarding a predetermined volume of water, which varied depending on the sampling port depth. Once collected in the syringes, porewater samples were taken to the surface.

Dissolved oxygen (DO) was measured in the field using an Orion 820 dissolved oxygen meter with a Clark-type electrode (Thermo Electron Corp., Beverly, MA, USA) while the sample was stirred continuously in a 20-mL Wheaton (Wheaton Industries Inc, Millville, NJ, USA) glass serum vial. The remaining porewater was filtered manually through pre-combusted

Whatman GF/F filters (47-mm diameter) with a nominal pore size of 0.7 µm (GE Healthcare, United Kingdom) held in plastic Millipore Swinnex filter holders (Millipore, Billerica, MA, USA), and frozen for later nutrient analysis.

All samples collected for dissolved inorganic nutrients were analyzed in duplicate for phosphate (PO_4^{3-}), silicate ($Si(OH)_4$), nitrite (NO_2^-), and in triplicate for total nitrate + nitrite (NO_x). Analytical triplicates were used when unreasonable differences were encountered between two replicates, and a Q-test was then used to determine whether or not to remove replicates (Skoog et al., 1994). The limits of detection for PO_4^3, $Si(OH)_4$, NO_2^- and NO_x were 0.26 µM, 0.48 µM, 14.6 nM and 0.32 µM, respectively. Although relatively high, these detection limits are quite adequate for porewater work.

Dissolved NO_2^- (± 7.4 nM) was determined by the formation of an azo dye (Grasshoff et al., 1983) and measured at 540 nm with a Shimadzu UV-1601 spectrophotometer (Shimadzu Scientific Instruments, Columbia, MD, USA) using a 10-cm cell. Both PO_4^{3-} (± 0.06 µM) and $Si(OH)_4$ (± 0.24 µM) were determined using the phosphomolybdate blue and siliciomolybdate blue methods (Grasshoff et al., 1983), respectively; a BioTek Synergy HT Multi-Mode Microplate Reader (BioTeck, Winooski, VT, USA) was used to measure spectrophotometrically PO_4^{3-} at 810 nm and $Si(OH)_4$ at 880 nm in Nunc 96 (Nalge Nunc International, Rochester, NY, USA) well optical bottom plates with a 1-cm pathlength.

Nitrate + nitrite (NOx) (± 0.18 µM) was determined using the nitrate reductase enzyme method (Campbell et al., 2006), after determining that it provided results comparable to the cadmium column method of Grasshoff et al. (1983) when used with porewater from our wells. Analytical triplicates were measured spectrophotometrically at 540 nm on a BioTek Synergy HT Multi-Mode Microplate Reader.

Dissolved inorganic carbon (DIC) samples were filtered with pre-combusted GF/F filters (described previously) and 20 ml were preserved using 50 µL of a saturated aqueous mercuric chloride solution (Dickson et al., 2007). Samples were stored at room temperature in pre-combusted, 20-mL Wheaton glass serum vials sealed with butyl rubber septa retained by crimp seals (Dickson et al., 2007). Samples for dissolved inorganic carbon (DIC) were collected on 25 November 2008, 2 December 2009, 18 December 2009 and 29 January 2010. DIC samples were analyzed in duplicate (± 0.02 mM) using a Model 5011 CO_2 Coulometer (UIC, Inc; Joliet, IL, USA).

Lastly, Mohr chlorinity titrations (Grasshoff et al., 1983) were used determine chlorinity and determine salinity with a precision of 0.4 %.

3.4 Data Corrections

Changes in sediment height at the porewater wells varied (± 3 cm) because of scouring or burial of the wells in the active environment at Kilo Nalu. Divers recorded the amount of scouring or burial of each porewater well in the field to ensure that the correct sampling depth below the SWI was recorded. Results reported here give the actual depth below the SWI, not the intended sampling depth.

Two types of corrections were applied to the porewater DO data. The first was an instrumental zero correction. Surface seawater collected from the south shore of Oahu was used to fill three-fourths of a 4-L glass reservoir in the laboratory. The top of the reservoir was sealed with a rubber stopper holding a gas sparger and a vent, while a port at the bottom was sealed with a rubber septum. To ensure the removal of all DO, the seawater was aerated with purified nitrogen gas for 30 min while the reservoir was stirred continuously with a large stirring bar. The Orion 820 dissolved oxygen meter was then used to measure DO in the seawater. The

lowest reading on the meter observed was 0.02 mg/L. This was considered the instrumental zero, and this correction was applied to the field data.

The second correction compensated for oxygen contamination of the porewater samples. This contamination resulted from oxygen-depleted porewater being held in semi-permeable plastic sampling syringes that were exposed to oxygen-saturated seawater and the atmosphere. Using the glass reservoir described above, syringes were used to mimic field sampling, with the exception of using a hypodermic needle at the end of the sampling tube, which pierced the reservoir's septum in order to collect a sample. Six samples from the reservoir were collected over 40 min, and the length of time between sample collection and measurement varied from 10 to 41 min. The syringes were rolled gently on a cart during this time to replicate motion from the sea swell during field operations. The meter was then used to measure DO exactly as it was done in the field. Contamination was found to increase logarithmically over time: $y = 0.2219\ln(t) + 0.0777$ (R^2 of 0.9732), where t is time (min) elapsed since sampling and y is the contamination (mg/L of DO). This correction was applied to the field porewater DO data. When values of t for individual sampling syringes were not available, average values from field records were used.

Instrument biofouling is often a concern in tropical waters with a large amount of light penetration. Although equipped with its own rubber wiper and copper faceplate to deter biofouling, significant biological growth occurred on the ECO FLNTU. Divers were therefore instructed to wipe the instrument's optical window whenever in the field. However, these measures were inadequate at times, resulting in an erroneously elevated fluorescence signal which had to be corrected.

Erroneous fluorescence signals were identified in the time-series records by a sudden drop in the fluorescence signal when a diver manually wiped the instrument's optical window. For example, a fluorescence signal resulting from biofouling occurred in September 2008 (Figure 3A). The biofouling was identified as occurring when typical fluorescence levels (Figure 3A; Symbol A) displayed a steadily increasing fluorescence signal, followed by a sudden drop in the signal after cleaning (Figure 3A; Symbol D).

For this particular event, two different biofouling periods were identified. Because of the natural, diurnal fluctuation in the fluorescence signal, a line was drawn for the first period, identified as A to B, using the daily minimum value in the fluorescence data; this was accomplished using MATLAB data processing software (The MathWorks, Inc., Natick, MA, USA). The fluorescence values for this line were subtracted from the measured data over the first biofouling period. The second biofouling period, identified as B to C, was adjusted the same way, with the signal at C being adjusted to the post-cleaning signal at D (Figure 3A). The resulting, corrected ECO FLNTU data are shown in Figure 3B.

3.5 Depth Integrations of Porewater Concentrations

Depth-integrated porewater concentrations were calculated using the Curve Fitting Toolbox, a part of MATLAB data processing software. All porewater concentrations were integrated to a depth of 50 cm below the SWI after applying a shape-preserving interpolant fit to the data.

4. Results

4.1 Sediment and Porewater Characterization

The uppermost sediments (hereafter used to describe the upper 10 cm) were determined to be >99 % sand. However, the deeper sediment has greater heterogeneity, with large coral

debris found at sediment depths of 15 cm and deeper. The estimated sediment organic content of the uppermost sediments, determined by loss-on-ignition, was 4.64% (SD = ± 0.11).

All DIC profiles peaked in the uppermost sediment (Figure 4), with maximum values of 2.3-2.5 mM, indicating that the highest sediment metabolism occurs in the uppermost sediment.

Previous porewater sampling conducted on two separate dates in 2006 indicated no salinity variation with sampling depth (Hebert et al., 2007). Samples collected and measured for chlorinity during this study were consistent with the previous findings, with all porewater salinities being within 0.5% (SD ± 0.4, n = 22) of that of the overlying water column (data not shown).

4.2 July-August 2008 Swell: Small Surface Gravity Wave Event

The goal of porewater sample collection in July and August 2008 was to capture variations in porewater profiles as a result of a surface gravity wave swell event. Significant wave heights and nearbed velocities for this time period, during which four sets of porewater samples were collected, are plotted in Figure 5. For the first two porewater collection dates, 23 and 25 July 2008, sampling occurred during background conditions with significant wave heights and nearbed velocities averaging 0.71 m and 0.19 m/s, respectively. The third set of samples was collected at the peak of the swell on 30 July 2008. At this time, significant wave heights reached 1.30 m, and nearbed velocities reached 0.35 m/s. The last porewater samples were collected on 6 August 2008 after conditions had returned to background levels; significant wave heights and nearbed velocities were 0.74 m and 0.19 m/s, respectively.

Throughout this sampling period for July and August 2008, PO_4^{3-} concentrations at the SWI averaged 0.27 µM (Figure 6 A-D). Sample collection during pre-swell background conditions showed enhanced PO_4^{3-} concentrations below the SWI, with a PO_4^{3-} maximum of ~3

µM at a depth of 9.5 cm. Similarly, during the background sample collections, average $Si(OH)_4$ concentrations at the SWI were 0.94 µM, with concentrations enhanced below the SWI interface; $Si(OH)_4$ also reached a maximum at ~9.5 cm during background conditions.

At the peak of the swell event, 30 July 2008, PO_4^{3-} and $Si(OH)_4$ concentrations in the 8-cm well nearly matched those of the overlying water column. Maximum PO_4^{3-} concentrations were still observed at 9.5 cm; however, maximum $Si(OH)_4$concentrations were found deeper in the sediment (17.2 µM at 20.5 cm). Porewater concentrations of NO_x and NO_2^- were enhanced over water-column concentrations for the July-August 2008 sampling dates except for the peak swell sampling point, 30 July 2008.

Bottom-water turbidity and fluorescence data for the July-August 2008 swell event are plotted in Figure 7. In the week prior to this swell event, mean turbidity was 0.42 NTU while fluorescence values had a mean of 56.5 counts. The three-day means for turbidity and fluorescence levels during the peak of the swell event were 1.05 NTU and 57.8 counts, respectively. The turbidity and fluorescence for the post-swell week had a mean of 0.40 NTU and 55.6 counts, respectively.

4.3 September 2008 Swell: Larger Surface Gravity Wave Event

The goal of sample collection in September 2008 was to capture variations in porewater profiles as a result of a larger surface-gravity wave event. Significant wave heights and nearbed velocities for this time period, during which four sets of porewater samples were collected, are plotted in Figure 8. The swell event first reached Kilo Nalu on September 4 and resulted in significant wave heights increasing from background values of 0.60 m to a maximum of 1.6 m. Similarly, nearbed velocities averaged 0.18 m/s before the swell event and were as high as 0.49

m/s during the event. Post-swell significant wave heights and nearbed velocities returned to background values, averaging 0.52 m and 0.15 m/s, respectively.

The first porewater samples were collected during background conditions on September 2 (Figure 8). Porewater samples collected on September 9 and 16 were taken during the swell event, which had two swell peaks. The first and larger peak reached its maximum on September 7, while the second peak crested on September 14 (Figure 8). Porewater samples collected on September 24 were collected after conditions had returned to background levels. The porewater profiles for 2, 9, 16 and 24 September 2008 are shown in Figure 9 A-D.

Corrected DO porewater concentrations on 24 September after the swell event were approximately zero at 8 cm depth, consistent with other background sampling. On September 9, on the tail of the larger swell peak, corrected DO concentrations at 8 cm depth were ~200 µM, matching those of the overlying water column. During the smaller swell peak, on September 16, corrected DO concentrations at 8 cm depth were 55 µM.

Both $Si(OH)_4$ and PO_4^{3-} collected during background conditions, September 2 and 24, showed enhancement over the overlying water column at the 8-cm depth and reached maximum concentrations by 15 cm below the SWI. However, lower concentrations of $Si(OH)_4$ and PO_4^{3-} were observed at 8 cm during the swell and waning-swell sample days, September 9 and 16 (Figure 9 B,C). Porewater concentrations of NO_x were enhanced over water-column concentrations on 2, 9 and 16 September 2008 (Figure 9), but NO_2^- concentrations varied in degree of enhancement throughout the swell event and reached a maximum during the waning swell (Figure 9).

Bottom-water turbidity and fluorescence data for the September 2008 event are plotted in Figure 10. Before the swell event, mean turbidity and fluorescence levels were 0.40 NTU

and 57.2 counts, respectively. The swell arrived 4 September 2008 and resulted in a four-day turbidity mean of 3.1 NTU, with a maximum turbidity of ~10 NTU during the peak of the swell on 7 September 2008. From 5-16 September 2008, a four-day mean fluorescence of 60.0 counts was maintained. Post-swell conditions resulted in a mean turbidity of 0.25 NTU, while mean fluorescence returned to 57.2 counts. Note that fluorescence concentrations during this swell period were corrected for biofouling (See Methods Section).

4.4 December 2008 Swell: Large Kona Swell Event

Unlike in July and September, porewater sampling in December 2008 occurred during a large Kona swell. This particular storm displayed large peaks in both wave height and freshwater input; while for the first two swell events, there was no appreciable freshwater input to the system. Significant wave heights and nearbed velocities for this event are plotted in Figure 11. The storm arrived on 10 December 2008, with significant wave heights reaching a maximum of 2.9 m on 11 December 2008, well above the average background conditions of 0.76 m observed during the two weeks prior. Nearbed velocity also peaked on 11 December 2008 at 0.64 m/s, compared to a background value of 0.16 m/s. A second peak the storm's intensity resulted in a maximum significant wave height of 2.4 m and maximum nearbed velocity of 0.48 m/s on 13 December 2008. Background conditions returned on 15 December 2008.

Each increase in swell was accompanied by an increase in freshwater input. Local rain gauges located at Aloha Tower (ALO) and in Mānoa Valley (MLA) (Figure 1) recorded 10.0 and 18.6 cm of rainfall, respectively, over ~18 hrs on 11 December 2008 (Figure 12). By 14 December 2008, 13.2 and 27.5 cm had fallen at ALO and MLA, respectively, during the three-day Kona storm (Figure 12). Prior to the storm, flow in the Mānoa-Pālolo Drainage Canal was

below estimated mean base flows. However, as the storm peaked on 11 December 2008, the highest flow of 2008 was reached, with the USGS 26247100 stream gauge (Figure 1) measured at 72 m^3/s, ~450 times mean base flow (Tomlinson et al., in prep. 2010). Freshwater input, measured at the WQB-AW and WQB-KN buoys (Figure 1) ~1 m below the surface, resulted in lowered ocean surface salinities, ~35 to 30.5 and 32.4, respectively (Figure 13). In the bottom water at Kilo Nalu, the freshwater signal was also observed, resulting in a drop in the salinity from 35.1 to 34.6, which was accompanied by a temperature drop of 0.7 °C (Figure 12).

Surface-water turbidity and fluorescence were collected ~1 m below the surface at the WQB-AW and WQB-KN Buoys. The two pulses of the storm are clearly evident in the turbidity record, with maxima at WQB-AW and WQB-KN of 14.0 and 6.6 NTU, respectively (Figure 14).

Bottom-water turbidity and fluorescence signals collected ~1 m above the SWI during this time period are plotted in Figure 15. The turbidity levels for the two weeks prior to the swell had a mean of 0.24 NTU, while fluorescence for the same period had a mean of 71.3 counts. The four-day means for turbidity and fluorescence during the peak of the storm were 4.5 NTU and 79.5 counts, respectively. At the storm's peak on 11 December 2008, turbidity levels were sustained above 20.0 NTU for several hours. After background conditions returned on 15 December 2008, the next 10 days resulted in a mean turbidity of 0.50 NTU, while the mean fluorescence was sustained at 79.5 counts.

Porewater sampling occurred during background conditions on 25 November 2008 and during the waning swell on 15 December 2008 (Figure 16). Although sampled 15 days prior to the swell, the 25 November 2008 sample is thought to be representative of background conditions before the swell. The mean V_{bed} from 25 November until when the swell arrived on

10 December was 0.16 (± 0.03 m/s), suggesting that physical conditions were largely constant over that period.

Porewater PO_4^{3-} concentrations on 25 November 2008 reached a maximum of 2.14 µM at 10.5 cm below the SWI, when $Si(OH)_4$ reached a maximum of 21.5 µM. On 15 December 2008, PO_4^{3-} was reduced by ~half to 1.05 µM while $Si(OH)_4$ was reduced by ~85% to 3.37 µM. Concentrations of NO_x at depth were slightly enhanced over SWI sample concentrations, and NO_2^- porewater concentrations were enhanced over water-column concentrations.

For both the background and the waning swell samples, corrected DO concentrations measured at the SWI were ~ 250 µM, with a concentration of ~ 0 µM at 10.5 cm (Figure 16). During background conditions, 25 November 2008, corrected DO concentrations showed increased DO deeper than 10.5 cm while samples collected 15 December 2008 showed no traces of DO below the SWI. DIC concentrations on 25 November 2008, were ~ 2 mM at the SWI and peaked at ~2.3 mM at 10.5 cm below the SWI. Conversely, corrected DO concentrations for that day reached a minimum at 10.5 cm; DIC concentrations mirrored DO concentrations throughout the depth profile (Figure 16A).

5. Discussion

5.1 Nutrient-nutrient Relationships

As organic matter undergoes remineralization, DIC and inorganic nutrients are produced (Froelich et al., 1979). During background conditions at Kilo Nalu, porewater DIC, PO_4^{3-} and $Si(OH)_4$ concentrations increase over concentrations found at the SWI. Respired dissolved inorganic nutrients, particularly PO_4^{3-} and $Si(OH)_4$, are linearly correlated with respired DIC (Figure 17). Respired concentrations are calculated by the increase in concentration of the remineralized endproduct above concentrations of the endproduct found at the SWI (respired X =

$X_{PW} - X_{SWI}$). Using the slopes from these plots of respired inorganic nutrients against respired DIC, we observe a molar inorganic carbon-to-phosphorus (C:P) ratio of 170 (R = 0.55) and a molar inorganic carbon-to-silicate (C:Si) ratio of 27.8 (R = 0.86) in the porewater.

5.1.1 C:P Relationship

Inorganic C:P ratios can be used to estimate the organic source matter undergoing remineralization in the sediment. We assume that the majority of the organic matter input deposited in the Kilo Nalu sediment is marine in origin, except in the case of intense localized storms (discussed below). The organic C:N:P ratio for coastal plankton off of Honolulu is 81:10.9:1 (Laws et al., 1984), while the median organic C:N:P ratio for benthic macroalgae and sea grasses is 550:30:1 (Atkinson and Smith, 1983). Using a 2-endmember mixing model with planktonic and benthic endmembers, and assuming an average C:P ratio for remineralization of 170 (Figure 17), the source organic matter to the sediments at Kilo Nalu was estimated to be 81% planktonic. This estimate assumes complete remineralization and ignores possible abiotic processes that can affect remineralized phosphate (e.g., Fox et al., 1986; Froelich, 1988) and is perhaps why the regression value for the C:P correlation is weak (R=0.55). C:N ratios would enhance the source matter calculation; however, total inorganic N cannot be computed without ammonium (NH_4^+) concentrations, which typically comprise a large portion of inorganic N in sediments. Ammonium concentrations are not available for the present study.

5.1.2 C:Si Relationship

The Si:DIC correlation (Figure 17) indicates that that the majority of Si in porewater results from organic matter remineralization. Deviation from the Si:DIC correlation could result if excess Si was abiotically added to the porewater. This is possible via submarine groundwater discharge to the sediment. However, the groundwater in Hawai‘i is highly enriched in dissolved Si (up to ~ 3.2

mM, Davis (1969)), derived from the dissolution of the silica-rich basaltic rock that forms the Hawaiian Islands. The Si:DIC correlation suggests that submarine groundwater discharge into the system is absent or negligible, which is consistent with the porewater chlorinity data (see Results). The strong correlation between $Si(OH)_4$ and DIC also indicates that planktonic and/or benthic diatoms may be major sources of organic matter to the sediment at Kilo Nalu, as diatoms are encased in silicate frustules that would be dissolved during remineralization.

5.2 Depth-integrated Porewater Concentrations

During the intensive sampling period from June to December 2008, eighteen sample sets were collected, including those during the three swell events described previously. The porewater nutrient profiles were numerically integrated to a depth of 50 cm to calculate depth-integrated concentrations for nutrients and oxygen. The depth-integrated concentrations of $Si(OH)_4$ and PO_4^{3-} for June to December 2008 are plotted in Figure 18.

5.2.1 Depth-integrated $Si(OH)_4$ Concentrations

From June to the beginning of September 2008, the depth-integrated concentration of $Si(OH)_4$ fluctuated around 400 µM. The depth-integrated concentration for $Si(OH)_4$ began to increase sharply at the end of September 2008, coinciding with the September 2008 south swell event. This depth-integrated $Si(OH)_4$ increase occurred without a corresponding increase in the depth-integrated concentrations of PO_4^{3-} (Figure 18).

A plot of $Si(OH)_4$ versus PO_4^{3-} (Figure 19) reveals two distinct types of organic matter being remineralized: one with a lower $Si:PO_4^{3-}$ ratio (2.8:1; $y = 2.8\ x + 2.9$, $R = 0.66$) and one with a higher $Si:PO_4^{3-}$ ratio (6.4:1; $y = 6.4\ x + 3.4$, $R = 0.70$) (Figure 19). The switch between trends coincides with the September 2008 swell event, suggesting that there was a shift then in the type of organic matter being remineralized in the sediment. The higher $Si:PO_4^{3-}$ ratio during the latter

period may reflect a greater proportion of diatoms being injected into the sediment and undergoing remineralization.

5.2.2 Depth-integrated DO and NO_x Concentrations

Porewater composition results from sediment metabolism , reflecting a balance between organic matter availability and viable electron acceptors (e.g., Froelich et al., 1979; Falter and Sansone, 2000b). Surface gravity waves can control the availability of viable electron acceptors by flushing the sediment with DO and other oxidants. Thus, porewater composition should vary with changes in wave height (Falter and Sansone, 2000b). This relationship is evident when examining the depth-integrated concentration of DO versus mean nearbed velocity for June to December 2008 (Figure 20). Mean nearbed velocity for this plot represents a mean of nearbed velocity from the data available for the six hours previous to porewater collection. This linear relationship suggests that an increase in nearbed velocity associated with increasing wave heights increases the rate of DO replenishment to the system to a level over the rate at which microbes consume DO during remineralization (Falter and Sansone, 2000b).

In contrast, we do not observe a strong relationship between depth-integrated NO_x concentrations and nearbed velocities (Figure 20). However, depth-integrated NO_x concentrations for June to December 2008 reveal a trend of higher total NO_x concentrations during the summer months of June through September (Figure 18). The summer months on the south shore of O‘ahu are dominated by south swells, and the increased wave heights result in enhanced fluid transport between the water column and porewater (Hebert et al., 2007). The oxygenation of the sediments may result in the oxidation of porewater NH_4^+ to NO_3^- (Jahnke, 2004), which would result in greater depth-integrated NO_x concentrations. Additionally, Grigg (1995) observed an increase in nitrate concentrations in the water column in Māmala Bay corresponding to increases in wave height (R^2 =

0.90). This relationship may have resulted from the buildup of NO_x due to sediment oxygenation, and the subsequent enhanced exchange of NO_x to the overlying water column during the swell events.

If an increase in swell size was the only variable affecting DO and NO_x concentrations, then one would expect the largest swells to result in the greatest amounts of depth-integrated DO and NO_x; however, this is not the case. During the largest of the swells, the Kona storm in December 2008, DO was not present ~10 cm below the SWI (Figure 16B). This event was unique because we observed not only the large swell heights and nearbed velocities, but also a large amount of freshwater with organic-matter runoff entering the system (Figures 11, 12 and 13) (Tomlinson et. al, in prep. 2010). The increase in the abundance of organic matter during this swell event could have caused an increase in sediment metabolism exceeding the amount DO and NO_3^- available, exhausting both these electron acceptors before progressing to a less energetically efficient pathways such as sulfate reduction (e.g., Froelich et al., 1979; Tribble et al., 1990).

The porewater sampling for the December 2008 event only captured a waning swell. During this period, the rate of exchange between the oxygenated water column and the sediments would have decreased from the rate during the peak of the swell event. Fram et al. (in prep., 2010) have shown that porewater in the uppermost sediments at Kilo Nalu can have residence times as short as a couple of hours when $H_{sig} \approx 1$ m, suggesting that nutrient concentrations will rebound quickly in the uppermost sediment after swell events. Yet, the sediment metabolism during the waning swell should still be enhanced over background levels, due to the additional organic matter injected during the swell event, causing depletion of available electron acceptors such as DO (Falter and Sansone, 2000b).

5.3 Porewater flushing and biological response to swell events

Surface gravity waves have been shown to be important in enhancing fluid exchange in permeable sediments (Shum, 1992; Haberstroh and Sansone, 1999; Falter and Sansone, 2000b; Boudreau et al., 2001). This effect was observed in both the July and September 2008 south swell events in our study. The flushing of the uppermost sediment during these events resulted in $Si(OH)_4$ and PO_4^{3-} concentrations in porewater matching those of the overlying water column (Figures 5C, 8 B and C). Additionally, for the September 2008 swell event, DO was fully replenished in the uppermost sediment during the swell event (Figure 9B). During the waning of the September 2008 swell, depletion of DO had already begun, decreasing to 55 µM in the uppermost sediment (Figure 9C).

Similarly, the December 2008 Kona swell event was characterized by a decrease in the porewater concentrations of $Si(OH)_4$ and PO_4^{3-} in the uppermost sediment during the waning swell. However, these concentrations were still elevated over SWI levels (Figure 9). This signature of lower enhanced dissolved nutrient concentrations and less depleted DO concentrations is likely a consequence of porewater sampling at the end of a swell event, reflecting renewed sediment metabolism in a recovering sediment, as discussed above.

A record of bottom-water turbidity and fluorescence for each swell event is available as proxies for particulate matter loading and biological productivity, respectively. Figure 21 shows multi-day turbidity and fluorescence means for pre-swell, swell and post swell conditions for the three swell events. Each swell showed an increase in turbidity during the swell event, followed by a return to background levels post-swell. This increased turbidity during the swell event was measured ~ 0.5 m from the SWI, suggesting that there was significant disturbance of the sediment at the SWI.

The corresponding increases in fluorescence (Figure 21) during the first two swell events (July and September) indicate that there was either an increase in biological productivity or that benthic phototrophs were suspended during the swell event. The fact that increased fluorescence levels were not sustained and quickly returned to ca. background levels during the post-swell conditions suggest that the suspended phototrophs had settled out or had penetrated through the SWI and were trapped in the sediment. Such filtration during the September swell event may have induced the shift in remineralized inorganic nutrient ratios seen after the September 2008 swell event (discussed previously).

The fluorescence level increase observed during the third and largest swell was maintained post-swell, suggesting a persistent photosynthetic response (Figure 21). A large amount of organic matter loading and freshwater also entered the system during this event, perhaps enhancing sediment metabolism; the enhanced flushing of the uppermost sediment during this event may have then increased inorganic nutrient transfer to the water column and brought about a photosynthetic response. It is more likely however, that the nutrients in the freshwater runoff that perturbed most of the water column (Figure 12) during the event may have contributed to sustaining a fluorescence response in the bottom water at Kilo Nalu.

6. Conclusions

Ratios of regenerated nutrients suggest that the majority of the organic matter undergoing respiration in the Kilo Nalu sediment is planktonic in origin. However, an apparent shift in source matter undergoing remineralization coincided with a late-summer swell event, suggesting that swell events and/or seasonality play a role in controlling the source matter for these sediments.

Increased nearbed velocities were correlated with greater depth-integrated DO concentrations, suggesting that a larger amount of DO is injected in the sediment with larger

significant wave heights and their correspondingly larger nearbed velocities. Seasonal variability in the physical environment appears to be linked to available amounts of NO_x in the sediment, with greater amounts available during the summer months, when the sediments are more aerated due to more intense austral winter wave action on the south shore of O‘ahu.

Swell events appear to enhance fluid exchange between the uppermost sediment and the overlying water column at Kilo Nalu, resulting in short time-scale variability of remineralized products such as dissolved inorganic nutrients. This short-term variability appears to be linked to changes in the physical environment, particularly surface gravity waves and nearbed velocities. The variability in the physical environment is also linked to bottom water particulate loads and fluorescence levels. The results from this study indicate that enhanced fluid exchange between the uppermost sediment and the overlying water column may represent an important input of inorganic nutrients to oligotrophic waters overlying permeable sediment in wave impacted nearshore environments. However, quantification of this enhanced fluid exchange is needed to confirm fluxes to the water column from the uppermost sediment.

7. References

Atkinson, M. J. and S. V. Smith (1983) C:N:P ratios of benthic marine plants. Limnology and Oceanography, 2: 568-574.

Boudreau, B. P., M. Huettel, S. Forster, R. A. Jahnke, A. McLachlan, J. J. Middelburg, P. Nielsen, F. J. Sansone, G. L. Taghon, W. Van Raaphorst, I. T. Webster, J. M. Weslawski, P. Wiberg and B. Sundby (2001) Permeable marine sediments: overturning an old paradigm. Eos, Transactions of the American Geophysical Union, 82: 133, 135-136.

Campbell, W. H. and P. Song (2006) Nitrate reductase for nitrate analysis in water. Environmental Chemistry Letters 4:69.

Davis, S.N. (1969) Silica in streams and ground water of Hawaii. Identification of Irrigation Return Water in the Subsurface. Technical Report No. 29.

Dickson, A.G., Sabine, C.L. and Christian, J.R. (Eds.) (2007). Guide to Best Practices for Ocean CO_2 Measurements. PICES Special Publication 3, 191 pp.

Emery and Thomson 2004. 2nd edition. Data Analysis Methods in Physical Oceanography. Elsevier. San Diego.

Falter, J. L. and F. J. Sansone (2000a) Shallow pore water sampling in reef sediments. Coral Reefs, 19: 93-97.

Falter, J. L. and F. J. Sansone (2000b) Hydraulic control of pore water geochemistry within the oxic-suboxic zone of a permeable sediment. Limnology and Oceanography, 45: 550-557.

Fletcher, C.H., E.E. Grossman, B.M. Richmond, and A.E. Gibbs (2002) Atlas of Natural Hazards in the Hawaii Coastal Zone. US Department of the Interior, US Geological Survey, Denver, CO: Geologic Investigations Series I-2761,182 pp.

Fox, L.E., S.L. Sager, and S.C. Wofsy (1986) The chemical control of soluble phosphorus in the Amazon estuary. Geochimica et Cosmochimica Acta, 50: 783-794.

Fram, J.P., F.J. Sansone and G. Pawlak (2010) Tracer advection in sandy sediment porewater under enhanced physical forcing. In prep.

Froelich, P.N., G.P. Klinkhammer, M.L. Bender. N.A. Luedtke. G.R. Heath, D. Cullen and P. Dauphin (1979) Early oxidation of organic matter in pelagic sediments of the eastern equatorial Atlantic: suboxix diagenesis. Geochimica et Cosmochimica Acta, 43: 1075-1090.

Froelich, P.N. (1988) Kinetic control of dissolved phosphate in natural rivers and estuaries: A primer on the phosphate butter mechanism. Limnology and Oceanography, 33: 649-668.

Fryer, P. (1995) The 1991-1992 NSF Young Scholars Program at the University of Hawai'i Science and Engineering Studies of the Ala Wai Canal, an Urban Estuary in Honolulu. Pacific Science, 49: 319-331.

Grasshoff, K., M. Ehrhardt, and K. Kremling (1983) Methods of Seawater Analysis. Verlag Chemie. New York, NY. 600 pp.

Grigg, R.W. (1995). Coral reefs in an urban embayment in Hawaii: a complex case history controlled by natural and anthropogenic stress. Coral Reefs, 14: 253-266.

Haberstroh, P. R. and F. J. Sansone (1999) Reef framework diagenesis across waveflushed oxic-suboxic-anoxic transition zones. Coral Reefs, 18: 229-240.

Hebert, A. B., F. J. Sansone, and G.R. Pawlak (2007) Tracer dispersal in sandy sediment porewater under enhanced physical forcing. Continental Shelf Reseach, 27, 2278-2287.

Huettel, M. and G. Gust (1992) Impact of bioroughness on interfacial solute exchange in permeable sediments. Marine Ecology Progress Series, 89: 253-267. 158

Huettel, M., W. Ziebis and S. Forster (1996) Flow-induced uptake of particulate matter in permeable sediments. Limnology and Oceanography, 41: 309-321.

Huettel, M., W. Ziebis, S. Forster and G.W. Luther III (1998). Advective transport affecting metal and nutrient distributions and interfacial fluxes in permeable sediments. *Geochimica et Cosmochimica Acta*, 62: 613-631

Huettel, M. and A. Rusch (2000) Transport and degradation of phytoplankton in permeable sediment. Limnology and Oceanography, 45: 534-549.

Jahnke, R. A. (2004) The Sea, Volume 13: Transport Processes and Organic Matter Cycling in Coastal Sediments, pp 163-192. *In* The Sea, Volume 13, The Global Coastal Ocean: Multiscale Interdisciplinary Processes by Allan R. Robinson. Harvard University Press, 1033 pp.

Jahnke, R. A., J. R. Nelson. R. L. Marinelli, and J. E. Eckman (2000) Benthic flux of biogenic elements on the Southeaster US continental shelf: influence of pore water advective transport and benthic microalgae. Continental Shelf Research, 20: 109-127.

Jahnke, R., M. Richards, J. Nelson, C. Robertson, A. Rao, and D. Jahnke (2005) Organic matter remineralization and porewater exchange rates in permeable South Atlantic Bight continental shelf sediments. Continental Shelf Research, 25: 1433-1452.

Laws, E.A., D.G. Redalje, L.W. Haas, P.K. Bienfang, R.W. Eppley, W.G. Harrison, D.M. Karl, and J. Marra (1984) High phytoplankton growth and production rates in oligotrophic Hawaiian coastal waters. Limnology and Oceanography, 29: 1161-1169.

Marinelli, R. L., R. A. Jahnke, D. B. Craven, J. R. Nelson and J. E. Eckman (1998) Sediment nutrient dynamics on the South Atlantic Bight continental shelf. Limnology and Oceanography, 43: 1305-1320.

Meyer-Reil, L.-A. (1986) Spatial and temporal distribution of bacterial populations in marine shallow water surface sediment, p. 141-160. *In* Lasserre, P. and J.M. 35

Moberly, R.J., and T. Chamberlain. (1964). Hawaiian Beach Systems. Honolulu, Hawaii: University of Hawaii, Hawaii Institute of Geophysics Technical Report No. 64-3, 95 p.

Reimers, C. E., H. A. Stecher III, G. L. Taghon, C. M. Fuller, M. Huettel, A. Rusch, N. Ryckelynck and C. Wild (2004) In situ measurements of advective solute transport in permeable shelf sands. Continental Shelf Research, 24: 183-201.

Riedl, R. J., N. Huang and R. Machan (1972) The subtidal pump: a mechanism of interstitial water exchange by wave action. Marine Biology, 13: 210-221.

Rocha, C. (2008). Sandy sediments as active biogeochemical reactors: compound cycling in the fast lane. Aquatic Microbial Ecology, 53: 119-127.

Rowe, G. T., C. H. Clifford, K. L. J. Smith and P. L. Hamilton (1975) Benthic nutrient regeneration and its coupling to primary productivity in coastal waters. Nature, 255: 215-217.

Rusch, A. and M. Huettel (2000) Advective particle transport into permeable sediments - evidence from experiments in an intertidal sandflat. Limnology and Oceanography, 45: 525-533.

Sansone, F. J., G. Pawlak, T. P. Stanton, M. A. McManus, B. T. Glazer, E. H. DeCarlo, M. Bandet, J. Sevadjian, K. Stierfhoff, C. Colgrove, A. B. Hebert, and I. C. Chen (2008) Kilo Nalu: physical/biogeochemical dynamics above and within permeable sediments. Oceanography, 12: 173-178.

Shum, K. T. (1992) Wave-induced advective transport below a rippled water-sediment interface. Journal of Geophysical Research, 97: 789-808.

Shum, K. T. and B. Sundby (1996) Organic matter processing in continental shelf sediments—the subtidal pump revisited. Marine Chemistry, 53: 81-87.

Skoog, West, Holler (1994) Analytical Chemistry: An Introduction. 6th edition. Saunders College Publishing. Philadelphia, 612 pp.

Tomlinson, M.S., E.H. De Carlo, M.A. McManus, G. Pawlak, G.F. Steward, F.J. Sansone, O.D. Nigro, C.E. Ostrander, R.E. Timmerman, J. Patterson, S. Jaramillo Uribé (2010) Monitoring the effects of storms on coastal water quality with the Hawai‘i Ocean Observing System (HiOOS) In prep.

Tribble, G. W., F. J. Sansone and S. W. Smith (1990) Stoichiometric modeling of carbon diagenesis within a coral reef framework. Geochimica et Cosmochimica Acta, 54: 2439-2449.

Webb, J. E. and J. Theodor (1968) Irrigation of marine submerged sands through wave action. Nature, 220: 682-683.

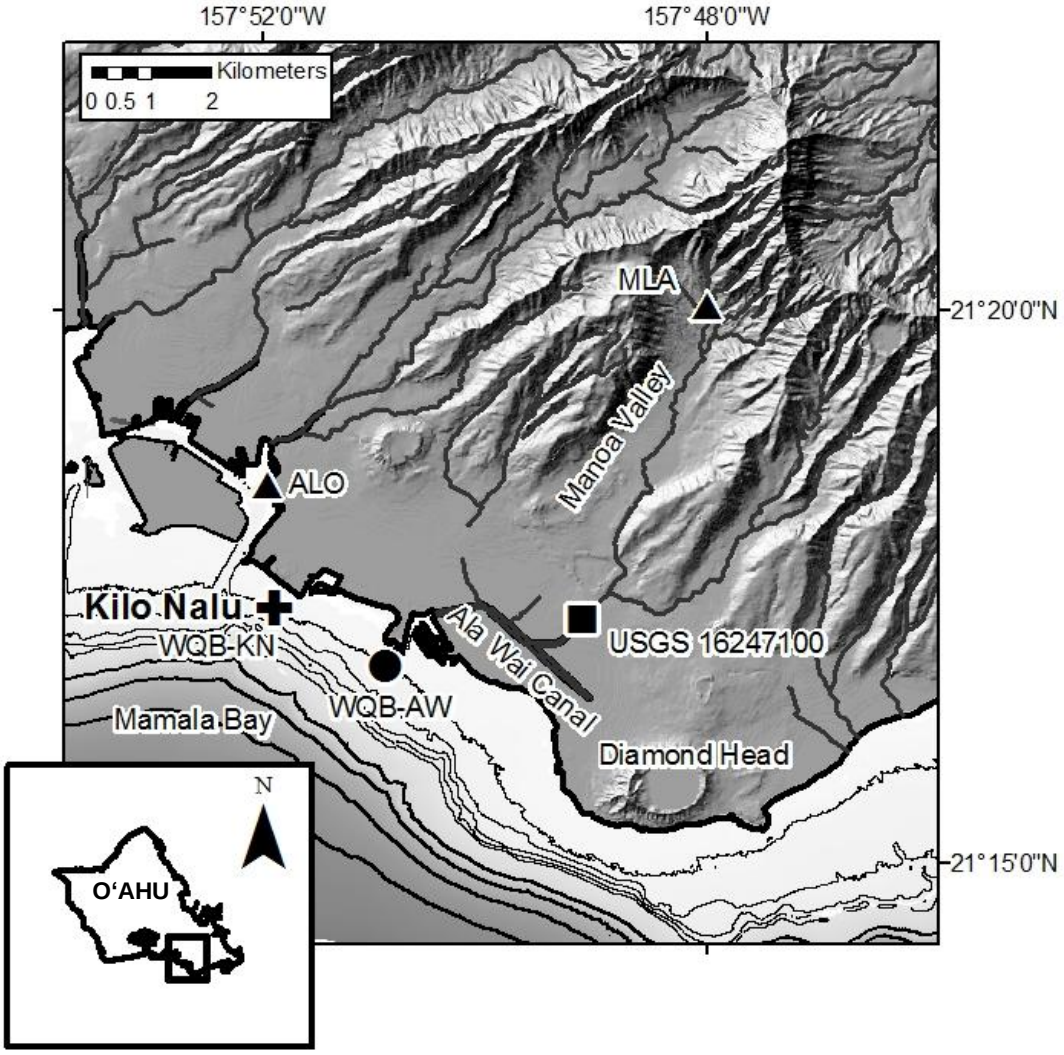

Figure 1: Map of Māmala Bay and southern Oʻahu, including the Ala Wai watershed. Kilo Nalu Observatory is indicated with a black cross. The two rain gauge sites, Mānoa Lyon Arboretum (MLA) and Aloha Tower (ALO), are indicated with black triangles, and USGS stream discharge gauge 16247100 is indicated with a black square. Water quality buoys are located south of the Ala Wai Canal (black circle) and at Kilo Nalu Observatory (black cross). Depth contours are shown every 10 m (thin black lines) and every 100 m (thick black lines) until 400 m.

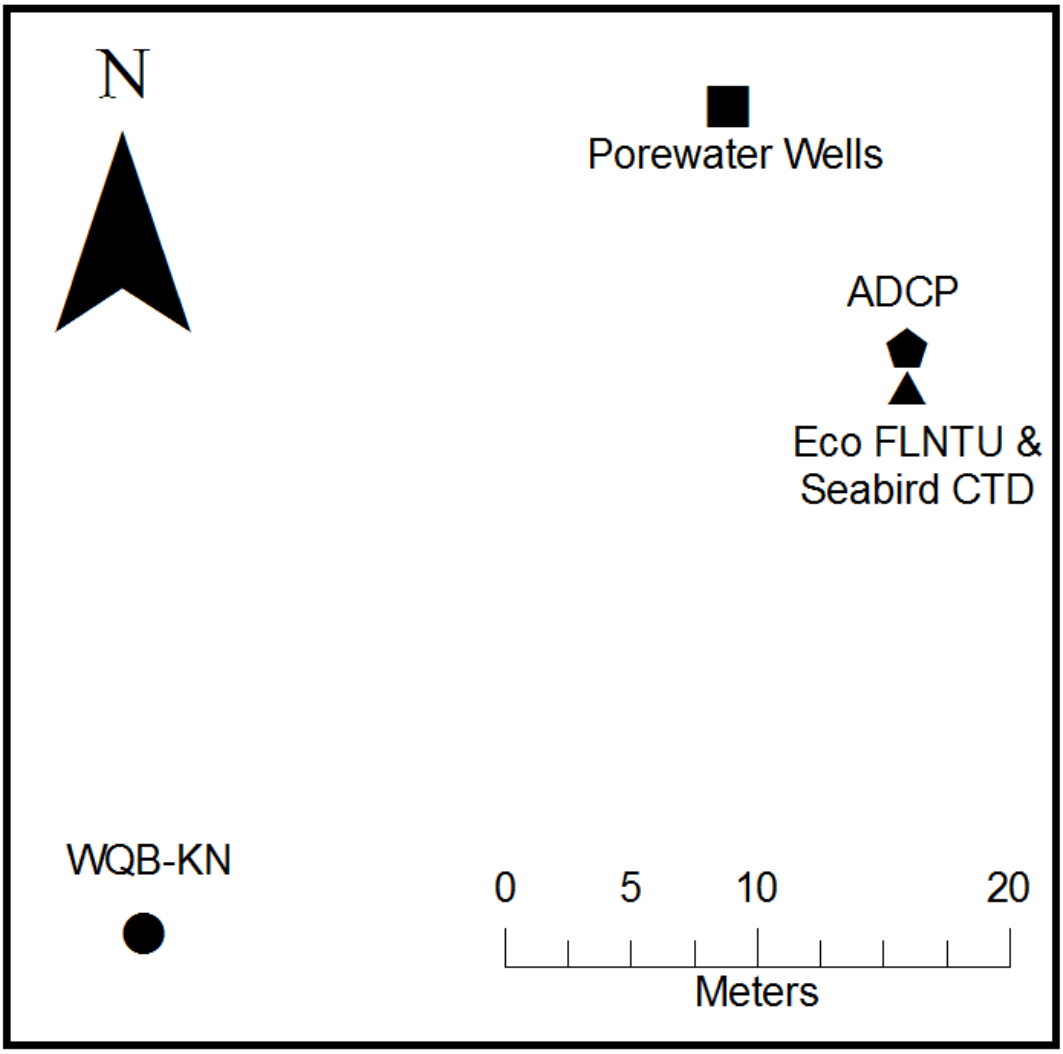

Figure 2: Map showing the location of instruments at Kilo Nalu Nearshore Observatory. Porewater wells, ADCP, Eco FLNTU and Seabird CTD are deployed at depth while Water Quality Buoy Kilo Nalu (WQB-KN) is deployed at the surface.

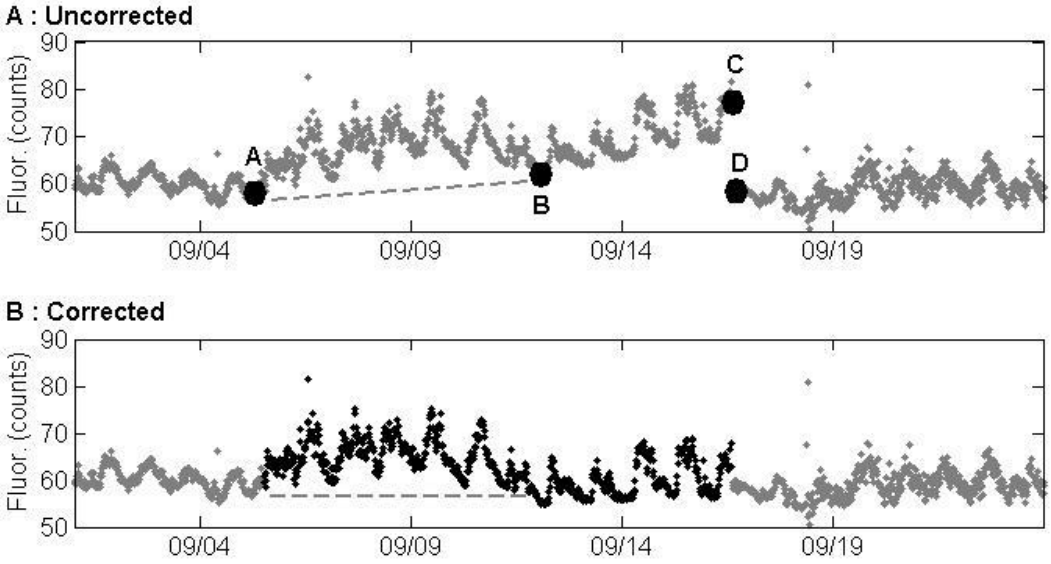

Figure 3: Top panel: bottom-water fluorescence data for 1 September to 24 September 2008 before correction for biofouling. Bottom panel: bottom-water fluorescence data for the same dates after biofouling correction (see text); corrected data are shown in black.

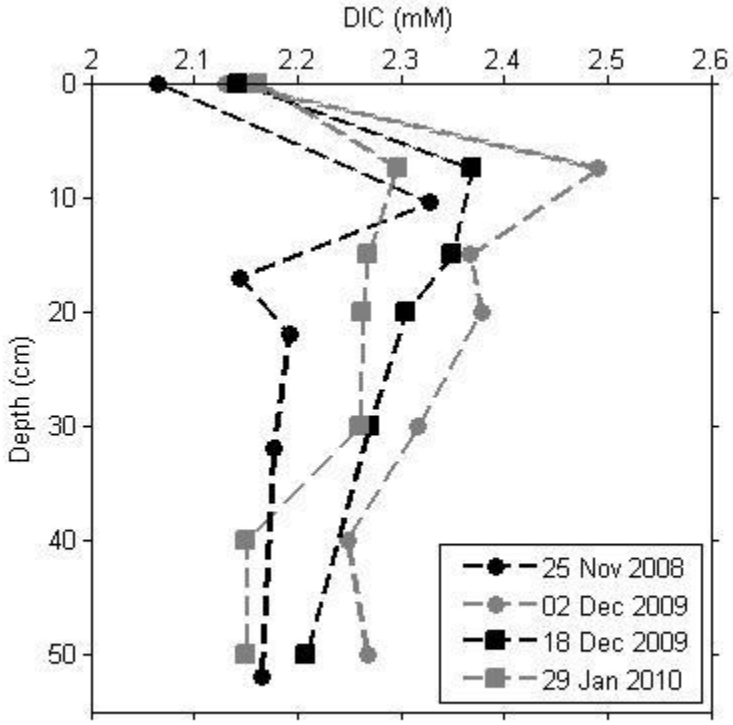

Figure 4: Porewater DIC concentrations for 25 November 2008, 2 December 2009, 18 December 2009 and 29 January 2010. In this and subsequent figures, values plotted at zero depth represent samples collected just above the SWI (see text).

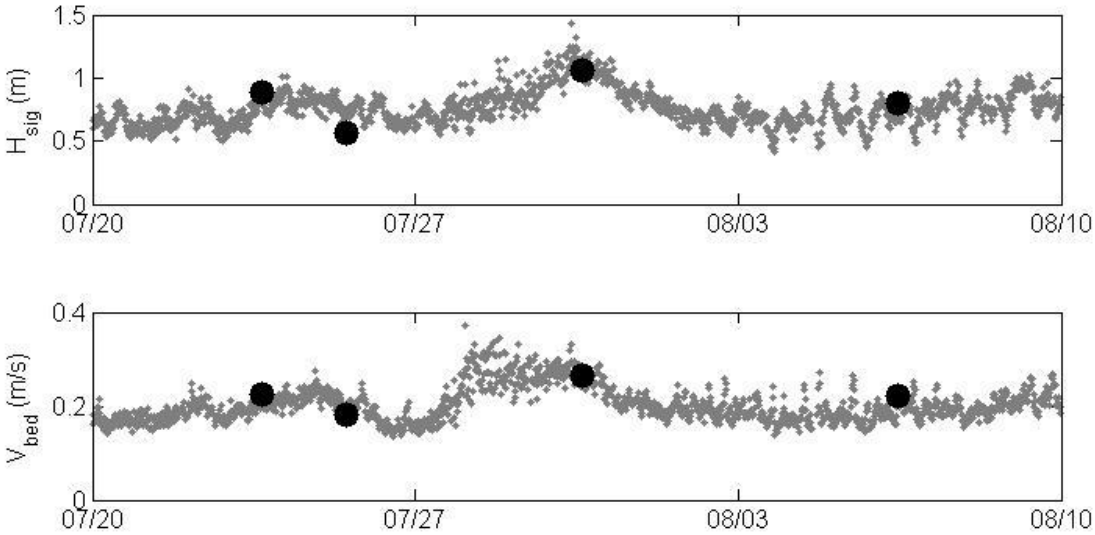

Figure 5: Top panel: significant wave heights from ADCP for 20 July 2008 to 10 August 2008. Bottom panel: nearbed velocities from ADCP for the same time period. Each point represents 20-min averaged data. Black circles indicate porewater sampling dates.

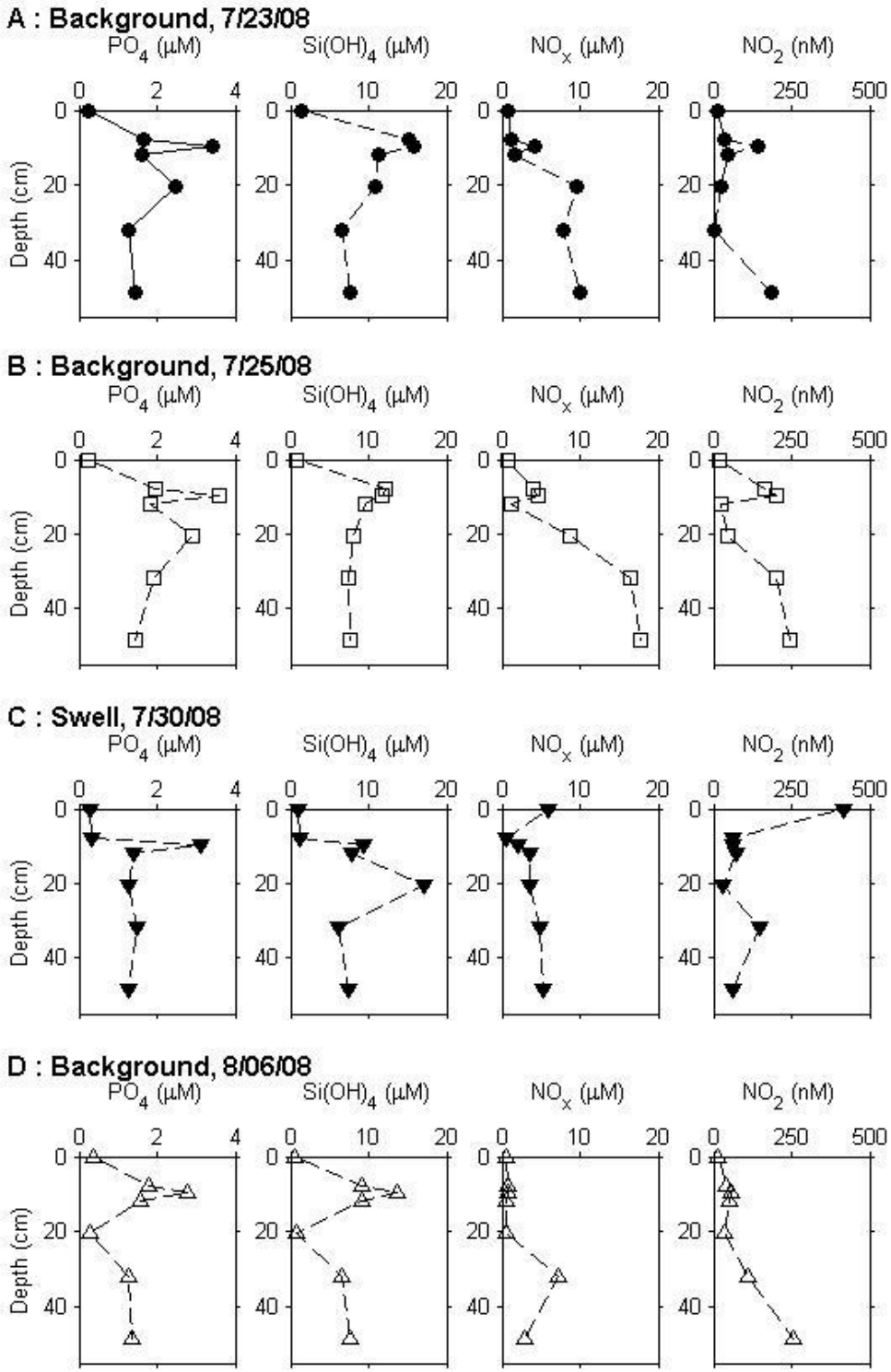

Figure 6: Porewater and SWI concentrations for PO_4, $Si(OH)_4$, NO_x and NO_2 during 23 July 2008 to 6 August 2008.

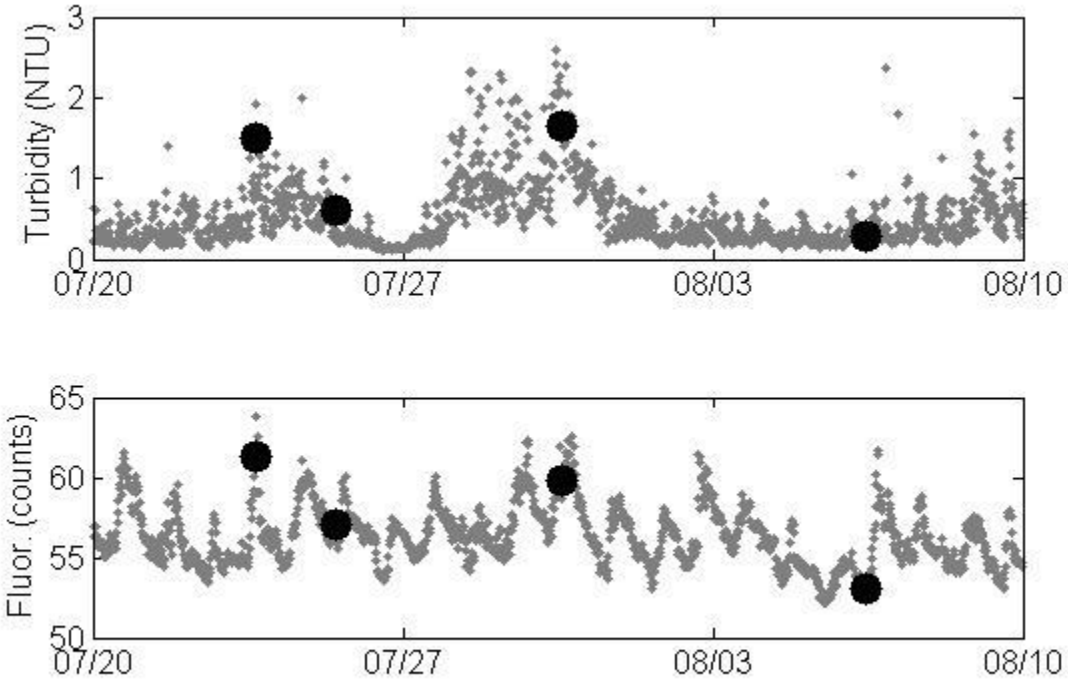

Figure 7: Top panel: bottom-water turbidity levels from ECO FLNTU. Bottom panel: bottom-water fluorescence levels from ECO FLNTU. Measurements are ~ 0.5 m above the SWI from 20 July 2008 to 10 August 2008. Each data point represents a 20-min average. Black circles indicate porewater sampling dates.

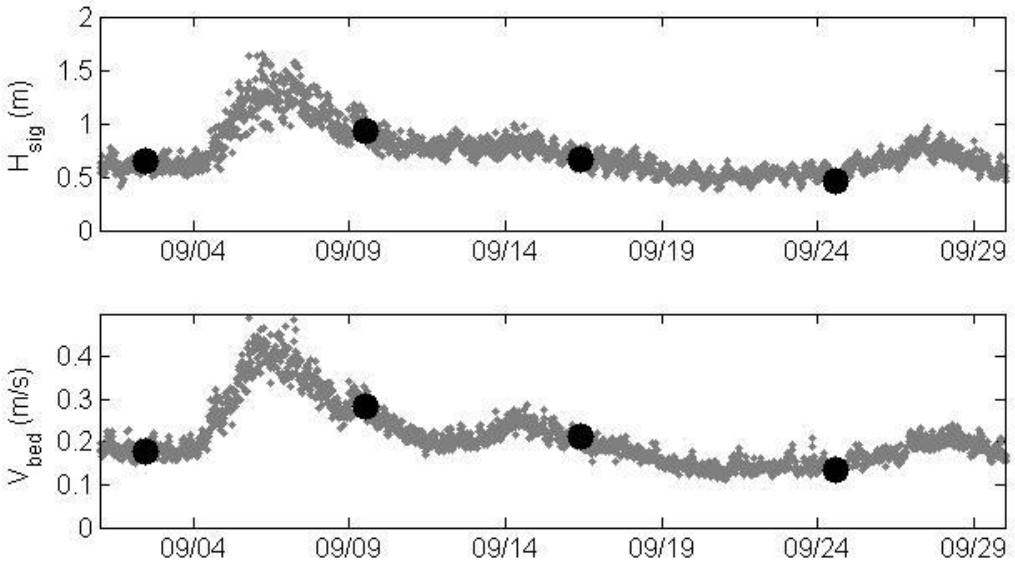

Figure 8: Top panel: significant wave heights from ADCP for 1 September to 30 September 2008. Bottom panel: nearbed velocities from ADCP for the same time period. Each point represents 20-min averaged data. Black circles indicate porewater sampling dates.

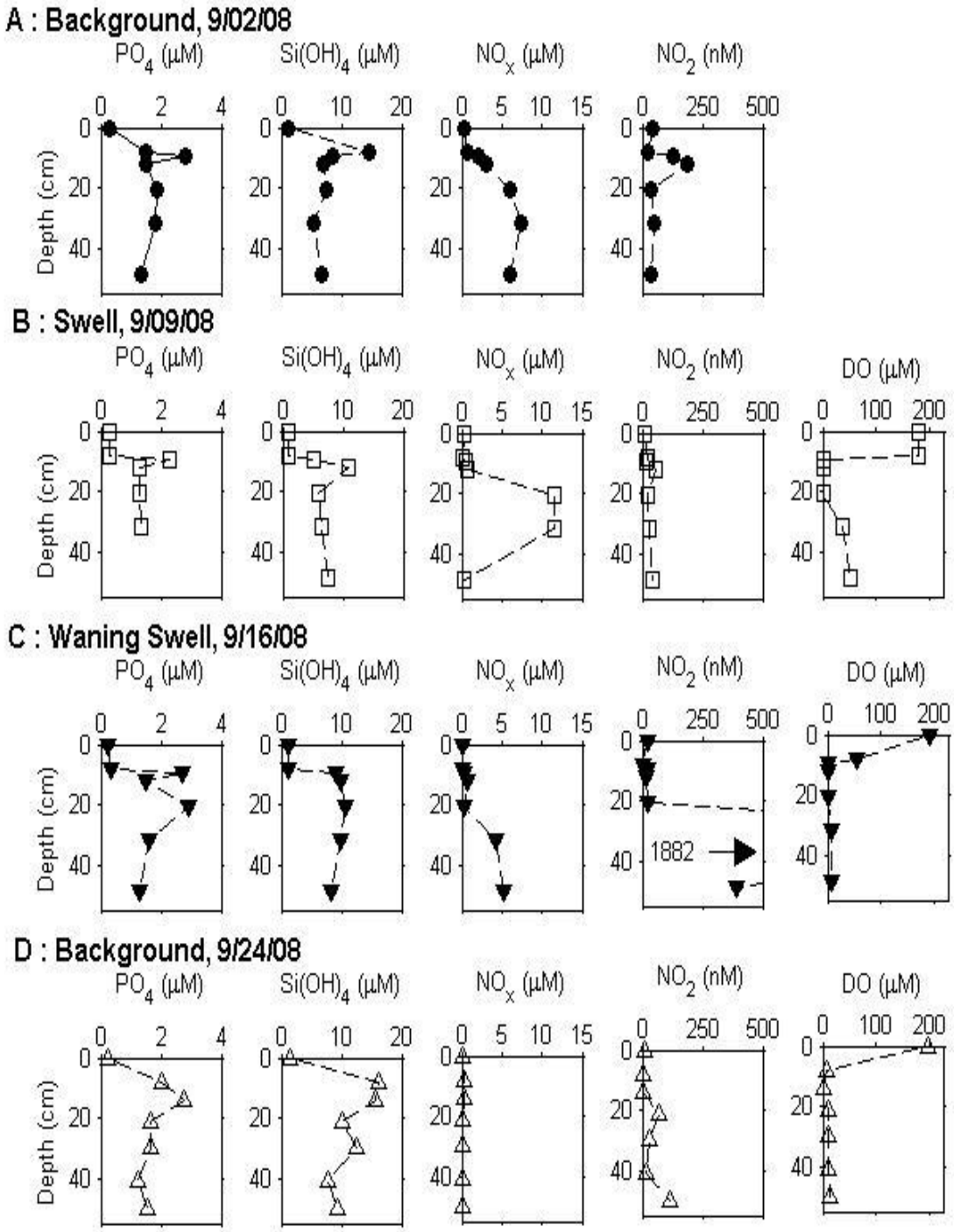

Figure 9: Porewater and SWI concentrations for PO_4, $Si(OH)_4$, NO_x, NO_2 and DO during 2 September 2008 to 24 September 2008. The 2 September SWI sampling is missing; values at 0 cm for this date represent the mean concentration from 25 sample dates.

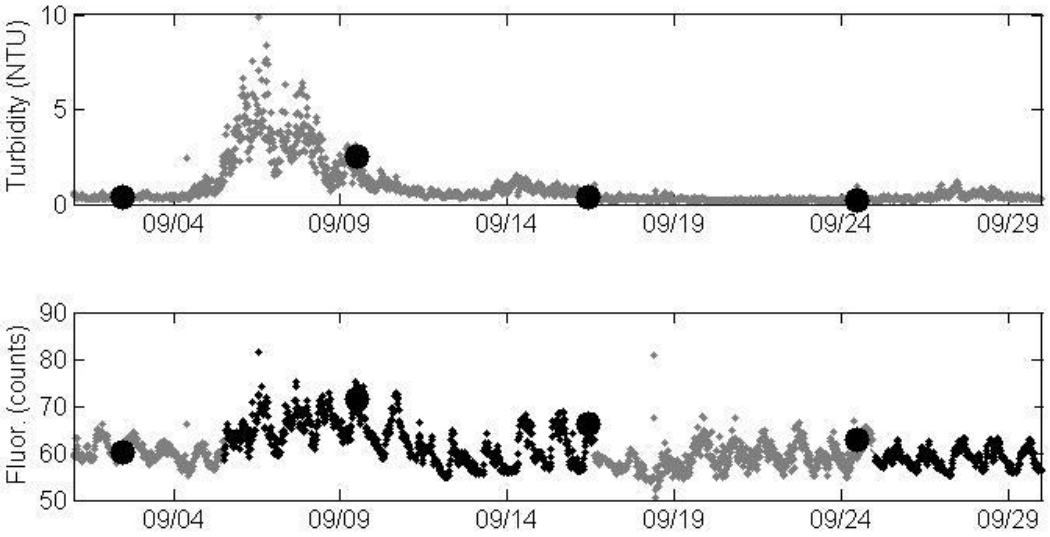

Figure 10: Bottom-water turbidity levels from ECO FLNTU (top panel) and bottom-water fluorescence levels from FLNTU (bottom panel), both taken ~0.5 m above the SWI from 4 August 2008 to 29 September 2008. Each data point represents a 20-min average. Black data points indicate that data has been corrected for biofouling (See Methods). Black circles indicate porewater sampling points.

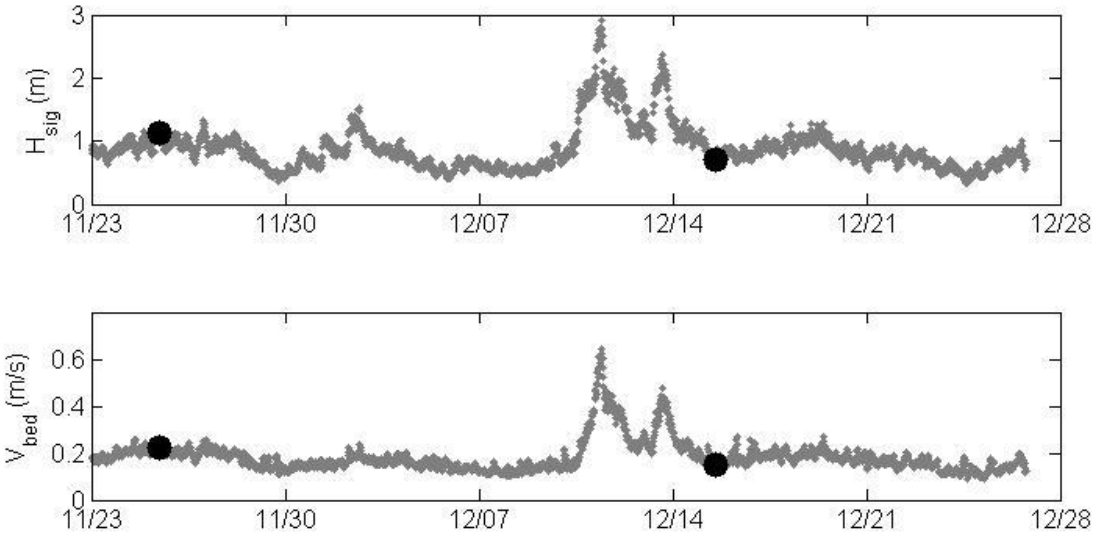

Figure 11: Top panel: significant wave heights from ADCP for 23 November 2008 to 28 December 2008. Bottom panel: nearbed velocities from ADCP for the same time period. Each point represents 20-min averaged data. Black circles indicate porewater sampling dates.

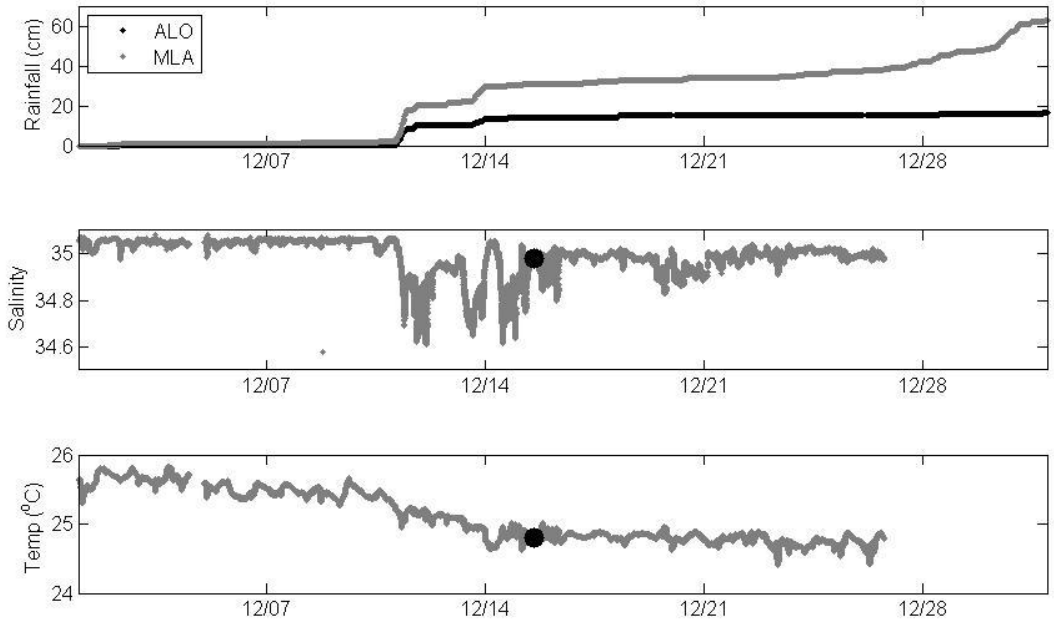

Figure 12: Top panel: cumulative rainfall from rain gauges starting 1 December 2008; Mānoa Lyon Arboretum (MLA) rain gauge data are shown in grey and Aloha Tower (ALO) rain gauge data are shown in black. Middle panel (bottom-water salinity from Seabird-37 CTD) and bottom panel (bottom-water temperature from Seabird-37 CTD), data were taken ~ 1 m above the SWI. Black circles indicate porewater sampling dates.

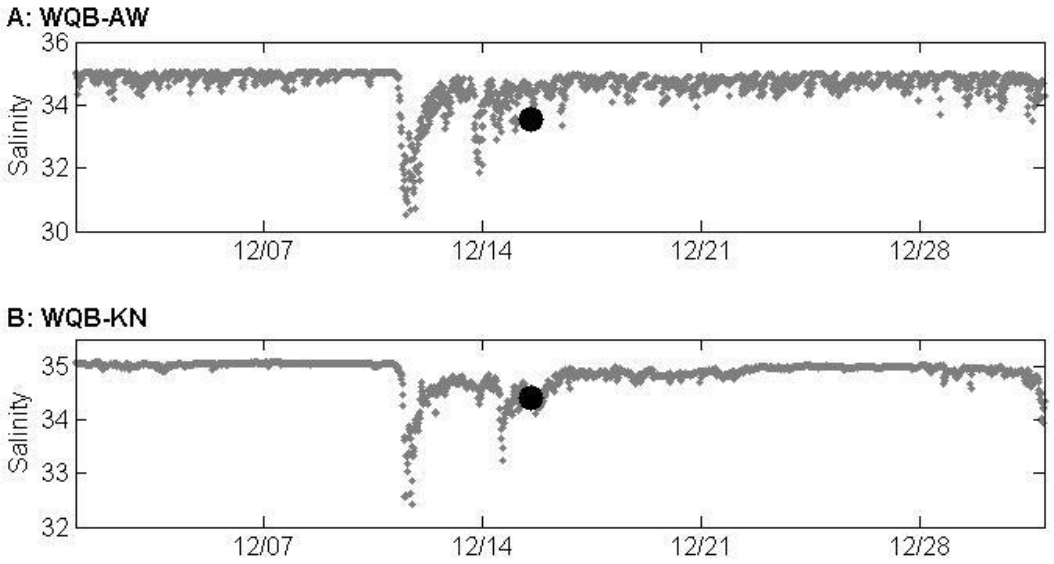

Figure 13: Top panel: surface salinity data from Seabird-16*plus* V2 SEACAT C-T collected at WQB-AW. Bottom panel: surface salinity data from Seabird-16*plus* V2 SEACAT C-T collected at WQB-KN. Data were collected ~1 m below the surface from 1 December to 31 December 2008. Note that salinity scales are different for each plot. Black circles indicate porewater sampling dates.

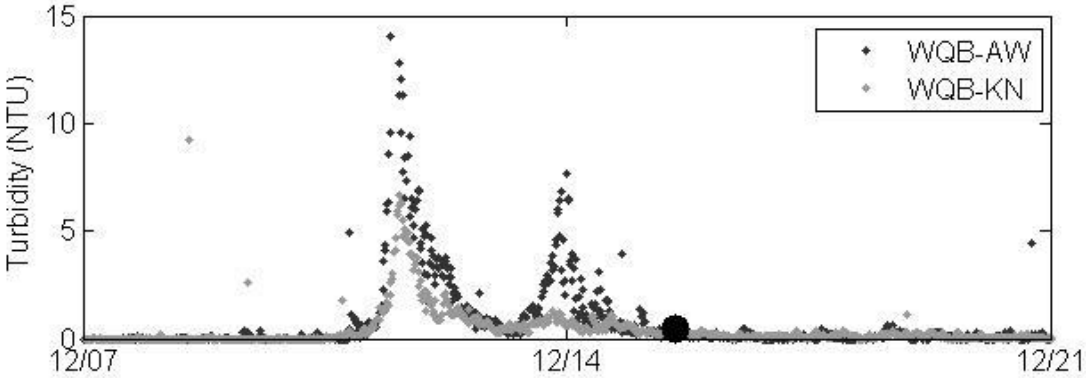

Figure 14: Surface turbidity levels from ECO FLNTUs measured at the WQB-AW (dark grey) and WQB-KN (light grey) buoys from 7 December 2008 to 21 December 2008. Black circle indicates porewater sampling date.

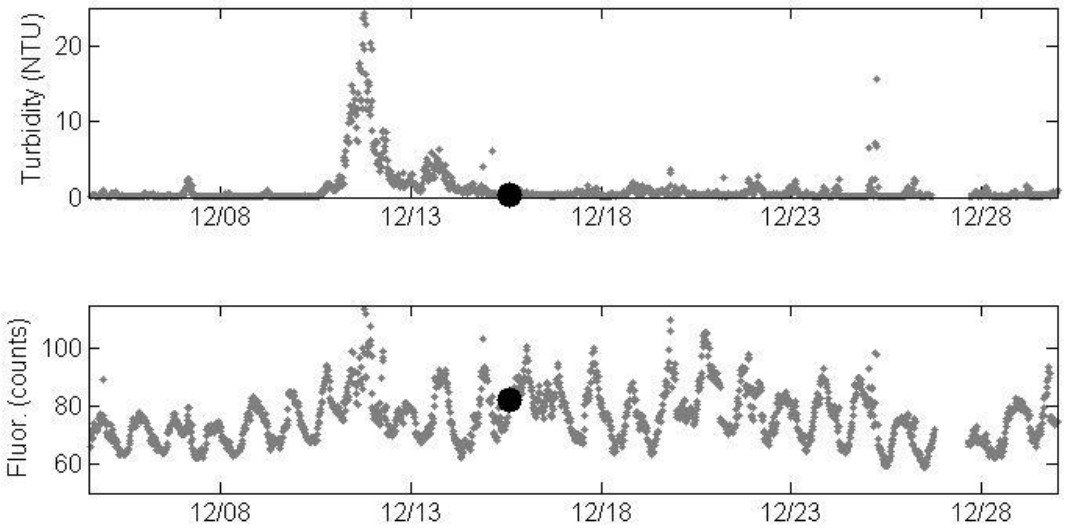

Figure 15: Top panel: bottom-water turbidity levels from ECO FLNTU. Bottom panel: bottom-water fluorescence levels from ECO FLNTU. Both were measured ~0.5 m above the SWI from 1 December to 31 December 2008. Each data point represents a 20-min average. Black circles indicate porewater sampling date.

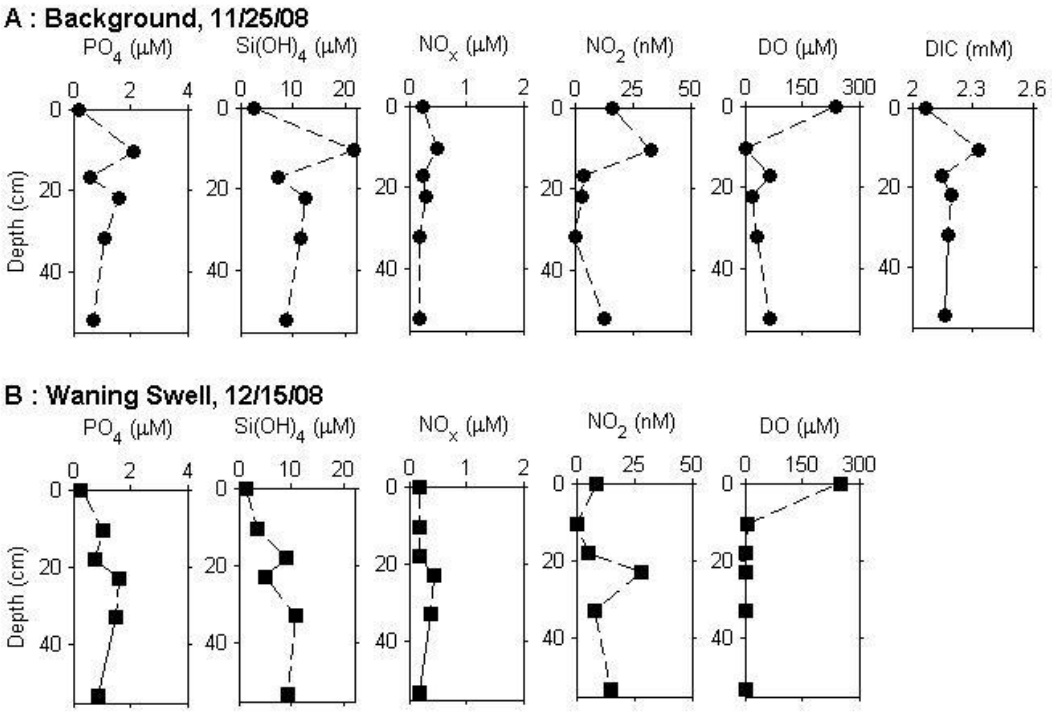

Figure 16: Porewater and SWI concentrations for PO_4, $Si(OH)_4$, NO_x, NO_2, DO and DIC at Kilo Nilo on 25 November 2008 and 15 December 2008. No DIC data was collected 15 December 2008.

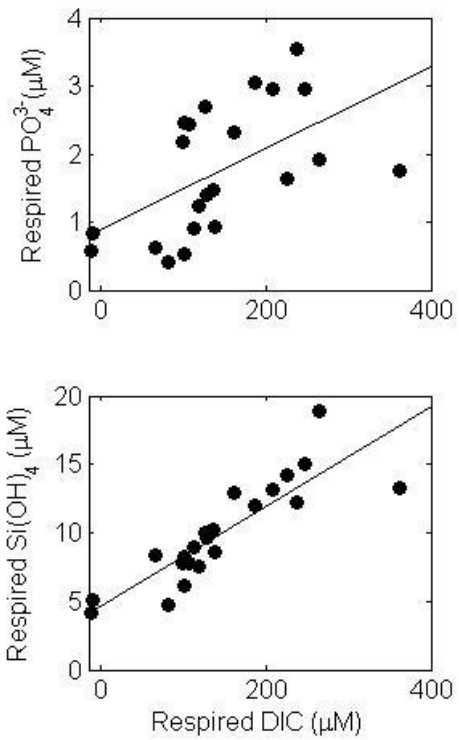

Figure 17: Respired PO_4^{3-} (top panel) and respired $Si(OH)_4$ (bottom panel) versus respired DIC. Respired values are porewater concentrations minus SWI concentration (respired $X = X_{PW} - X_{SWI}$).

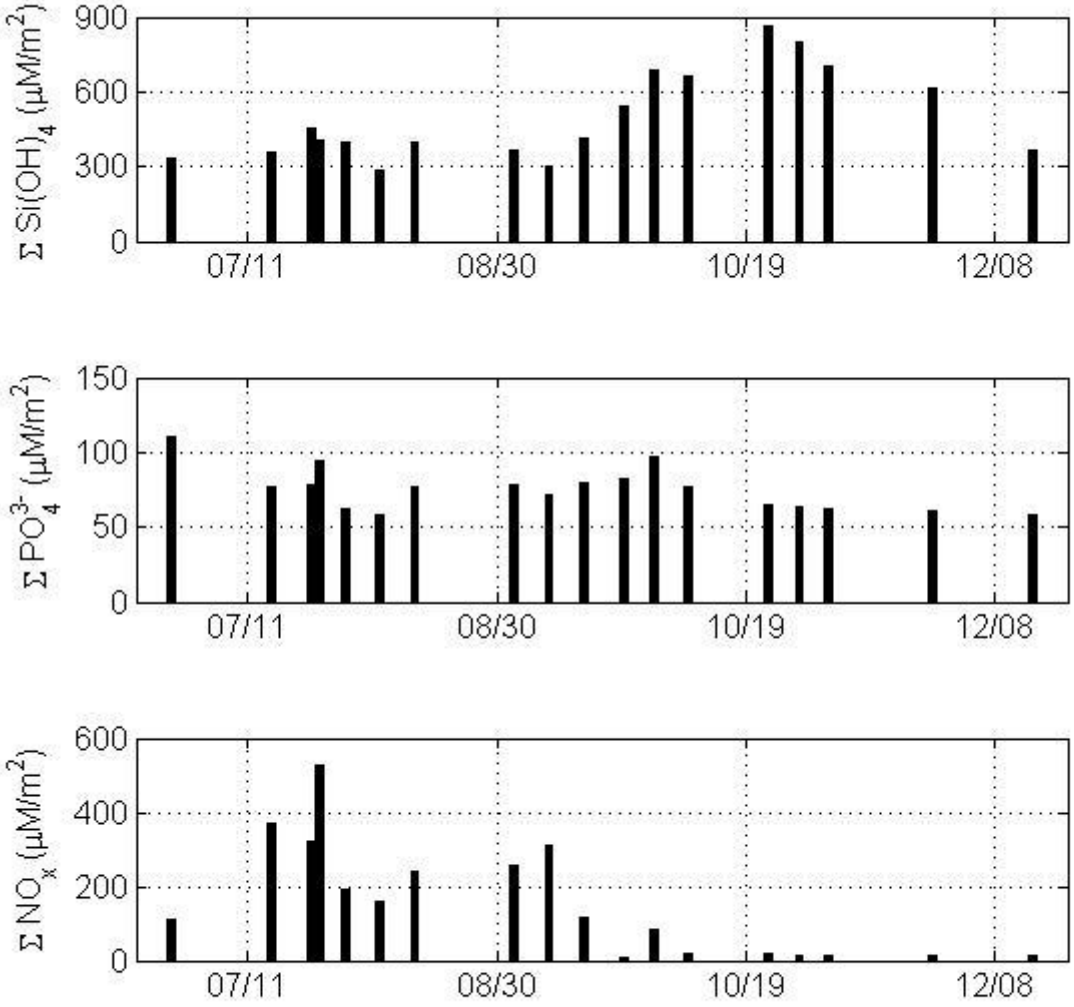

Figure 18: Top panel: depth-integrated $Si(OH)_4$ porewater concentrations. Middle panel: depth-integrated PO_4 porewater concentrations. Bottom panel: depth-integrated NO_x porewater concentrations. All are for June to December 2008.

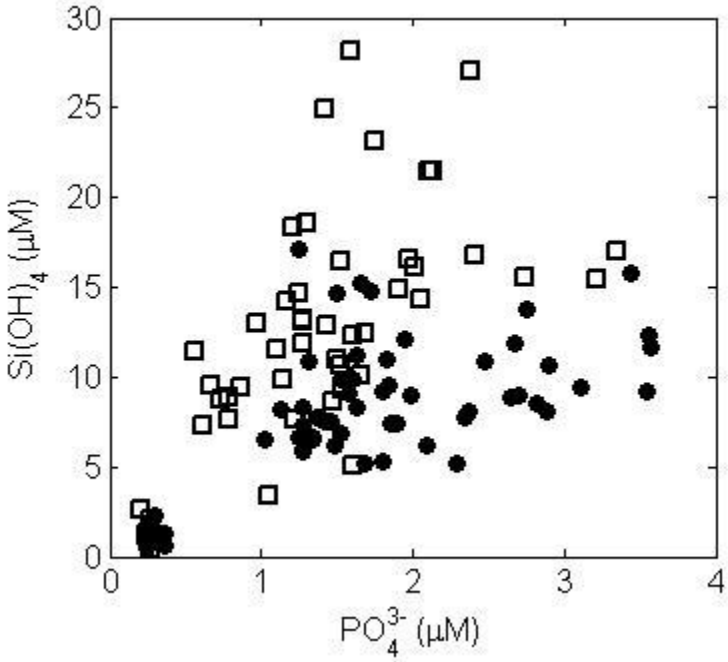

Figure 19: Porewater $Si(OH)_4$ concentrations versus PO_4^{3-} concentrations for porewater samples collected from June to December 2008. Closed circles represent samples collected prior to the September swell event (y = 2.8 x + 2.9, R = 0.66), and open squares represent samples collected after the September 2008 swell event (y = 6.4 x + 3.4, R = 0.70).

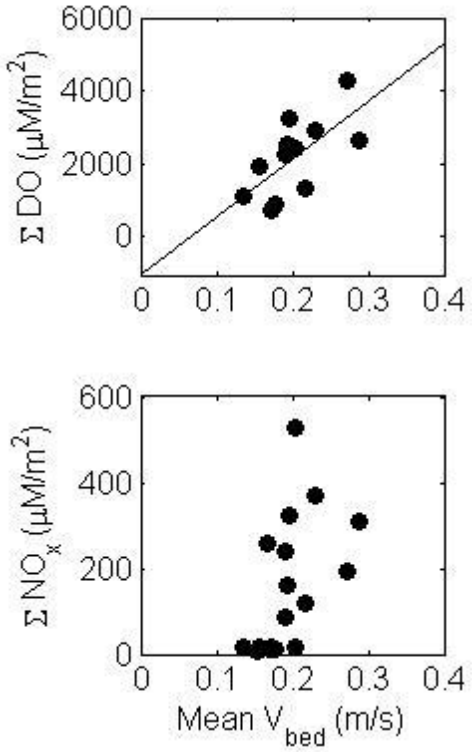

Figure 20: Top panel: depth-integrated porewater concentration of DO versus mean nearbed velocity; line is y = 15975x-1067.6, R = 0.67. Bottom panel: depth-integrated porewater concentration of NO_x versus mean nearbed velocity. Mean nearbed velocities used in these correlations were calculated using velocities from the 6 hours prior to porewater sampling. Data collected June to December 2008.

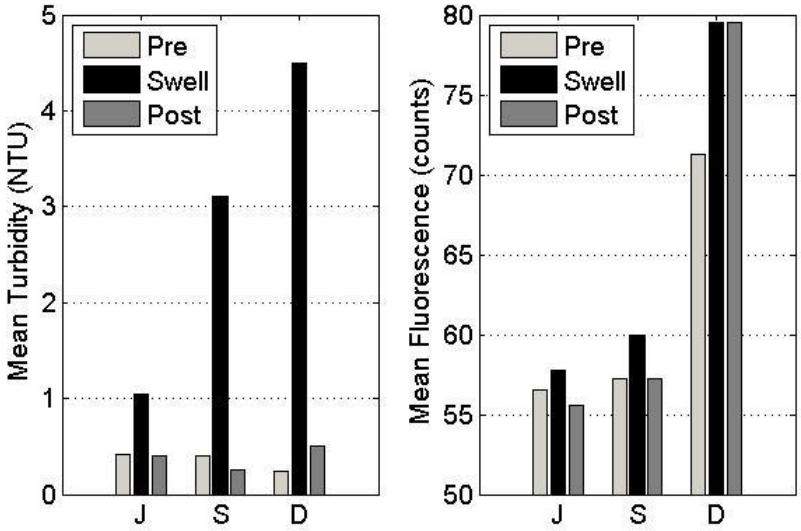

Figure 21: Multi-day mean for bottom-water turbidity and fluorescence levels from ECO FLNTU for July (J), September (S) and December (D) 2008 swell events. Light grey = pre-swell means, black = swell means, and dark grey = post-swell means.

Appendix A

Inorganic nutrient, dissolved oxygen, dissolved inorganic carbon and iron data for porewater collected 26 August 2007 to 29 January 2010. DIN is a total of nitrate, nitrite and ammonium. Ammonium concentrations are considered minimum estimates due to compromising of samples before ammonium analysis. Iron was measured using the ferrozine method and represents Fe^{2+}. Actual sampling depths have been corrected for the burial or scouring of porewater wells. DO concentrations represent corrected values (see Methods Section).

Date	Intended Depth (cm)	Actual Depth (cm)	NOx (µM)	NO_2^- (nM)	NH_4^+ (µM)	DIN (µM)	PO_4^{3-} (µM)	$Si(OH)_4$ (µM)	DIC (mM)	DO (µM)	Fe (µM)
8/26/07	0	0	N/A	N/A	N/A	N/A	N/A	N/A	N/A	N/A	N/A
	7.5	8	0.0	20.4	0.3	0.3	1.7	10.4	N/A	N/A	N/A
	15	14	0.0	83.1	0.4	0.4	2.0	9.9	N/A	N/A	N/A
	20	21	0.0	93.7	0.4	0.4	1.3	2.7	N/A	N/A	N/A
	30	29.5	0.0	57.9	0.4	0.4	1.5	5.8	N/A	N/A	N/A
	40	41	0.0	5.2	0.2	0.2	0.9	4.9	N/A	N/A	N/A
	50	50	0.0	30.0	0.6	0.6	0.5	4.0	N/A	N/A	N/A
8/31/07	0	0	0.0	0.0	0.2	0.2	0.4	0.2	N/A	N/A	N/A
	7.5	8	0.3	39.7	1.1	1.4	2.1	7.5	N/A	N/A	N/A
	15	14	1.8	24.4	1.4	3.2	2.8	9.1	N/A	N/A	N/A
	20	21	0.0	96.9	0.0	0.0	1.2	2.0	N/A	N/A	N/A
	30	29.5	4.9	45.4	0.2	5.1	1.6	5.1	N/A	N/A	N/A
	40	41	5.8	18.8	0.3	6.0	0.9	4.7	N/A	N/A	N/A
	50	50	0.0	63.2	0.7	0.7	1.0	3.8	N/A	N/A	N/A
9/4/07	0	0	0.0	0.0	0.4	0.4	0.3	0.3	N/A	N/A	N/A
	7.5	8	0.0	2.1	1.6	1.6	2.8	9.9	N/A	N/A	N/A
	15	14	1.2	39.6	3.6	4.8	2.7	9.6	N/A	N/A	N/A
	20	21	0.0	221.4	0.7	0.7	1.2	3.1	N/A	N/A	N/A
	30	29.5	7.4	25.4	0.5	7.9	1.3	4.9	N/A	N/A	N/A
	40	41	6.5	1.0	0.4	6.9	0.8	4.9	N/A	N/A	N/A
	50	50	5.3	62.0	0.5	5.8	0.9	4.1	N/A	N/A	N/A
9/20/07	0	0	N/A	24.6	0.9	0.9	0.3	0.7	N/A	184.1	N/A
	7.5	8	N/A	13.0	0.8	0.8	1.9	5.7	N/A	5.9	N/A
	15	14	N/A	66.3	0.8	0.8	2.9	11.4	N/A	0.0	N/A
	20	21	N/A	120.0	0.8	0.8	1.4	5.3	N/A	5.6	N/A
	30	29.5	N/A	38.0	0.8	0.8	1.5	7.0	N/A	34.6	N/A
	40	41	N/A	2.1	0.8	0.8	0.9	5.4	N/A	78.3	N/A
	50	50	N/A	23.4	0.8	0.8	0.9	4.3	N/A	76.2	N/A

Date	Intended Depth (cm)	Actual Depth (cm)	NOx (µM)	NO_2^- (nM)	NH_4^+ (µM)	DIN (µM)	PO_4^{3-} (µM)	$Si(OH)_4$ (µM)	DIC (mM)	DO (µM)	Fe (µM)
11/20/07	0	0	0.1	0.0	1.1	1.1	0.3	0.4	N/A	N/A	N/A
	7.5	8	0.4	0.0	2.2	2.6	1.7	18.3	N/A	N/A	N/A
	15	14	0.1	4.9	1.0	1.1	3.4	11.5	N/A	N/A	N/A
	20	21	0.0	17.0	0.9	0.9	1.7	8.7	N/A	N/A	N/A
	30	29.5	2.4	67.4	0.8	3.2	2.3	8.3	N/A	N/A	N/A
	40	41	0.0	72.3	0.8	0.8	0.7	4.5	N/A	N/A	N/A
	50	50	4.1	128.7	0.8	4.9	1.1	6.4	N/A	N/A	N/A
1/25/08	0	0	0.0	0.0	0.8	0.8	0.3	1.2	N/A	N/A	N/A
	7.5	8	0.1	2.9	0.9	1.0	0.8	10.4	N/A	N/A	N/A
	15	14	0.4	66.3	6.3	6.7	1.8	7.7	N/A	N/A	N/A
	20	21	0.1	0.0	2.1	2.2	1.8	8.6	N/A	N/A	N/A
	30	29.5	1.3	11.6	0.8	2.1	3.0	9.3	N/A	N/A	N/A
	40	41	7.2	14.0	1.1	8.3	1.0	7.0	N/A	N/A	N/A
	50	50	5.6	0.0	0.8	6.3	1.3	6.7	N/A	N/A	N/A
4/16/08	0	0	0.1	1.5	0.9	1.0	0.3	2.0	N/A	N/A	N/A
	7.5	8	N/A	N/A	N/A	N/A	N/A	N/A	N/A	N/A	N/A
	15	14	0.2	17.6	0.8	1.0	2.5	11.3	N/A	N/A	N/A
	20	21	0.1	0.9	0.7	0.8	1.5	8.5	N/A	N/A	N/A
	30	29.5	0.0	0.0	0.9	0.9	2.0	8.1	N/A	N/A	N/A
	40	41	0.2	0.0	0.8	1.0	0.9	6.6	N/A	N/A	N/A
	50	50	0.2	0.0	0.7	0.9	0.8	5.5	N/A	N/A	N/A
6/25/08	0	0	N/A	N/A	N/A	N/A	N/A	N/A	N/A	N/A	N/A
	7.5	8	0.7	15.2	1.0	1.6	1.1	8.2	N/A	N/A	N/A
	15	9.5	0.7	106.6	0.9	1.6	3.6	12.3	N/A	N/A	N/A
	20	12	0.7	34.5	0.8	1.5	2.0	9.0	N/A	N/A	N/A
	30	20.5	7.7	41.0	0.9	8.6	2.6	8.9	N/A	N/A	N/A
	40	32	0.9	49.2	1.0	1.9	1.7	5.1	N/A	N/A	N/A
	50	48.5	1.0	251.5	1.1	2.0	4.5	7.1	N/A	N/A	N/A

Date	Intended Depth (cm)	Actual Depth (cm)	NOx (µM)	NO_2^- (nM)	NH_4^+ (µM)	DIN (µM)	PO_4^{3-} (µM)	$Si(OH)_4$ (µM)	DIC (mM)	DO (µM)	Fe (µM)
7/15/08	0	0	8.5	427.6	2.8	11.3	0.3	2.3	N/A	191.9	N/A
	7.5	8	6.0	547.7	0.9	6.9	1.8	10.9	N/A	22.4	N/A
	15	9.5	8.6	477.9	0.8	9.5	3.5	9.2	N/A	8.1	N/A
	20	12	8.5	458.0	0.8	9.3	1.3	6.0	N/A	10.3	N/A
	30	20.5	11.7	894.7	0.9	12.6	2.4	8.1	N/A	41.4	N/A
	40	32	1.2	235.7	0.8	2.0	1.0	6.5	N/A	67.3	N/A
	50	48.5	16.1	904.4	0.8	16.9	2.1	6.2	N/A	67.8	N/A
7/23/08	0	0	0.7	13.1	1.0	1.7	0.2	1.4	N/A	172.5	N/A
	7.5	8	1.2	36.6	2.8	4.0	1.7	15.2	N/A	0.0	N/A
	15	9.5	4.2	139.6	2.5	6.7	3.4	15.7	N/A	0.6	N/A
	20	12	1.6	48.2	6.8	8.4	1.6	11.2	N/A	0.0	N/A
	30	20.5	9.6	24.6	0.9	10.5	2.5	10.8	N/A	35.2	N/A
	40	32	7.9	2.3	0.9	8.8	1.3	6.5	N/A	66.7	N/A
	50	48.5	10.1	184.5	1.1	11.2	1.4	7.6	N/A	23.4	N/A
7/25/08	0	0	0.7	17.1	0.5	1.2	0.2	0.8	N/A	N/A	N/A
	7.5	8	3.9	161.7	4.3	8.2	2.0	12.1	N/A	N/A	N/A
	15	9.5	4.6	203.9	4.5	9.1	3.6	11.6	N/A	N/A	N/A
	20	12	1.1	23.9	5.3	6.4	1.8	9.6	N/A	N/A	N/A
	30	20.5	8.6	44.9	3.5	12.1	2.9	8.1	N/A	N/A	N/A
	40	32	16.3	198.9	8.7	25.0	1.9	7.4	N/A	N/A	N/A
	50	48.5	17.6	242.2	3.4	21.0	1.5	7.5	N/A	N/A	N/A
7/30/08	0	0	6.0	414.4	3.4	9.4	0.3	0.9	N/A	203.8	N/A
	7.5	8	0.6	60.0	1.1	1.7	0.3	1.3	N/A	99.9	N/A
	15	9.5	2.1	60.4	2.4	4.5	3.1	9.5	N/A	16.9	N/A
	20	12	3.6	71.1	6.5	10.0	1.4	7.8	N/A	28.4	N/A
	30	20.5	3.5	30.2	0.8	4.3	1.3	17.2	N/A	110.5	N/A
	40	32	4.8	147.1	1.6	6.3	1.5	6.2	N/A	59.5	N/A
	50	48.5	5.3	63.1	0.8	6.1	1.3	7.3	N/A	79.4	N/A

Date	Intended Depth (cm)	Actual Depth (cm)	NOx (µM)	NO_2^- (nM)	NH_4^+ (µM)	DIN (µM)	PO_4^{3-} (µM)	$Si(OH)_4$ (µM)	DIC (mM)	DO (µM)	Fe (µM)
8/6/08	0	0	0.5	16.1	0.7	1.3	0.4	0.6	N/A	208.1	N/A
	7.5	8	0.7	37.7	1.0	1.7	1.8	9.2	N/A	10.9	N/A
	15	9.5	0.8	55.4	5.8	6.5	2.8	13.7	N/A	5.0	N/A
	20	12	0.5	49.9	3.6	4.1	1.6	9.1	N/A	0.0	N/A
	30	20.5	0.5	37.4	0.7	1.3	0.3	0.8	N/A	162.1	N/A
	40	32	7.2	110.4	0.8	8.0	1.3	6.6	N/A	8.6	N/A
	50	48.5	2.9	254.5	0.8	3.7	1.4	7.7	N/A	12.2	N/A
8/13/08	0	0	0.5	15.5	0.7	1.3	0.2	0.4	N/A	N/A	N/A
	7.5	8	0.5	27.6	1.1	1.6	1.7	14.8	N/A	10.5	N/A
	15	9.5	1.2	168.8	3.1	4.3	2.7	11.9	N/A	0.0	N/A
	20	12	0.6	110.3	2.3	2.9	1.6	8.4	N/A	5.3	N/A
	30	20.5	6.0	96.5	0.8	6.8	2.3	7.7	N/A	18.3	N/A
	40	32	7.3	17.0	0.8	8.1	1.3	6.6	N/A	34.5	N/A
	50	48.5	6.5	49.1	0.8	7.3	1.3	6.5	N/A	29.7	N/A
9/2/08	0	0	N/A	N/A	N/A	N/A	N/A	N/A	N/A	N/A	N/A
	7.5	8	0.7	21.2	1.1	1.8	1.5	14.7	N/A	N/A	N/A
	15	9.5	2.1	125.8	4.3	6.4	2.8	8.5	N/A	N/A	N/A
	20	12	3.1	190.1	1.0	4.1	1.5	6.9	N/A	N/A	N/A
	30	20.5	6.1	37.0	0.8	6.9	1.9	7.4	N/A	N/A	N/A
	40	32	7.4	50.7	27.9	35.3	1.8	5.3	N/A	N/A	N/A
	50	48.5	6.0	37.1	0.9	6.9	1.3	6.6	N/A	N/A	N/A
9/9/08	0	0	0.3	11.8	1.4	1.7	0.3	1.0	N/A	180.3	N/A
	7.5	8	0.2	20.4	1.0	1.2	0.3	0.9	N/A	177.8	N/A
	15	9.5	0.4	19.2	2.6	3.0	2.3	5.1	N/A	0.0	N/A
	20	12	0.7	53.1	4.5	5.2	1.3	10.9	N/A	0.0	N/A
	30	20.5	11.5	22.9	1.7	13.2	1.3	5.9	N/A	0.0	N/A
	40	32	11.5	27.2	1.7	13.2	1.3	6.5	N/A	35.6	N/A
	50	48.5	0.3	40.8	5.6	5.9	N/A	7.5	N/A	53.0	N/A

Date	Intended Depth (cm)	Actual Depth (cm)	NOx (µM)	NO_2^- (nM)	NH_4^+ (µM)	DIN (µM)	PO_4^{3-} (µM)	$Si(OH)_4$ (µM)	DIC (mM)	DO (µM)	Fe (µM)
9/16/08	0	0	0.2	20.2	1.1	1.3	0.2	1.2	N/A	192.2	N/A
	7.5	8	0.0	0.0	1.0	1.0	0.4	1.3	N/A	54.0	N/A
	15	9.5	0.4	25.6	4.3	4.7	2.7	9.0	N/A	0.0	N/A
	20	12	0.7	18.0	1.7	2.4	1.5	9.9	N/A	0.0	N/A
	30	20.5	0.2	26.3	2.0	2.3	2.9	10.6	N/A	0.0	N/A
	40	32	4.2	1822.5	1.3	5.5	1.6	9.8	N/A	7.9	N/A
	50	48.5	5.2	392.8	0.8	6.1	1.3	8.4	N/A	6.9	N/A
9/24/08	0	0	0.1	7.2	N/A	0.1	0.2	1.3	N/A	196.8	N/A
	7.5	8	0.2	0.0	1.0	1.2	2.0	16.1	N/A	6.4	N/A
	15	14	0.3	0.0	0.8	1.0	2.7	15.6	N/A	0.2	N/A
	20	21	0.2	68.0	0.7	0.9	1.7	10.0	N/A	11.8	N/A
	30	29.5	0.2	29.3	0.7	0.9	1.7	12.5	N/A	10.9	N/A
	40	41	0.1	13.9	0.9	1.0	1.2	7.7	N/A	11.0	N/A
	50	50	0.1	115.9	0.8	0.9	1.5	9.3	N/A	12.0	N/A
9/30/08	0	0	0.4	14.2	0.4	0.8	0.3	1.3	N/A	198.1	N/A
	7.5	6.5	0.7	17.1	0.4	1.0	2.1	21.5	N/A	31.3	N/A
	15	13	0.5	0.0	0.4	0.9	3.3	17.0	N/A	29.1	N/A
	20	20	0.4	0.0	0.4	0.8	1.4	12.9	N/A	45.9	N/A
	30	30	0.9	32.6	0.4	1.3	2.4	16.8	N/A	30.9	N/A
	40	40	4.7	57.1	0.6	5.3	1.5	8.6	N/A	44.4	N/A
	50	49	3.0	46.0	0.4	3.4	1.5	10.6	N/A	33.4	N/A
10/7/08	0	0	0.2	0.0	0.8	1.0	0.3	0.8	N/A	178.4	N/A
	7.5	7	0.5	0.0	0.7	1.2	1.7	23.2	N/A	23.1	N/A
	15	12	0.7	0.0	0.7	1.4	3.2	15.5	N/A	22.2	N/A
	20	20	0.3	20.2	0.9	1.2	1.3	13.1	N/A	25.0	N/A
	30	29.5	0.3	48.7	0.8	1.1	1.9	14.9	N/A	26.9	N/A
	40	41	0.3	10.4	0.9	1.2	0.8	7.6	N/A	44.4	N/A
	50	48	0.3	0.0	0.9	1.2	1.1	9.9	N/A	41.6	N/A

Date	Intended Depth (cm)	Actual Depth (cm)	NOx (µM)	NO_2^- (nM)	NH_4^+ (µM)	DIN (µM)	PO_4^{3-} (µM)	$Si(OH)_4$ (µM)	DIC (mM)	DO (µM)	Fe (µM)
10/23/08	0	0	0.4	8.8	0.8	1.2	0.3	2.0	N/A	186.7	N/A
	7.5	10.5	0.4	14.0	0.8	1.2	1.6	28.2	N/A	0.0	N/A
	15	18	0.4	43.9	0.9	1.3	2.0	16.6	N/A	0.0	N/A
	20	23	0.2	10.0	1.1	1.3	1.3	18.6	N/A	0.0	N/A
	30	33	0.3	137.3	0.9	1.2	1.2	14.2	N/A	0.0	N/A
	40	43	N/A	N/A	N/A	N/A	N/A	N/A	N/A	N/A	N/A
	50	53	0.4	20.0	1.0	1.4	1.3	14.7	N/A	0.0	N/A
10/29/08	0	0	0.2	0.1	0.7	0.9	0.3	1.7	N/A	206.7	N/A
	7.5	10.5	0.2	52.7	0.8	0.9	2.4	27.1	N/A	0.0	N/A
	15	18	0.3	33.4	0.8	1.1	1.2	18.4	N/A	0.0	N/A
	20	23	0.2	33.0	0.8	1.1	1.5	16.5	N/A	0.0	N/A
	30	33	0.2	0.0	0.8	1.0	1.0	13.0	N/A	0.0	N/A
	40	43	N/A	N/A	N/A	N/A	N/A	N/A	N/A	N/A	N/A
	50	53	0.3	12.4	1.0	1.2	0.6	11.4	N/A	15.2	N/A
11/4/08	0	0	0.2	0.4	0.8	1.0	0.3	0.4	N/A	N/A	N/A
	7.5	10.5	0.3	21.2	0.9	1.2	1.4	25.0	N/A	N/A	N/A
	15	18	0.2	9.5	0.8	1.0	1.3	13.2	N/A	N/A	N/A
	20	23	0.3	32.7	0.8	1.2	2.1	14.4	N/A	N/A	N/A
	30	33	0.2	0.0	0.9	1.1	1.3	11.8	N/A	N/A	N/A
	40	43	N/A	N/A	N/A	N/A	N/A	N/A	N/A	N/A	N/A
	50	53	0.2	41.2	0.9	1.1	0.7	9.5	N/A	N/A	N/A
11/25/08	0	0	0.2	15.5	N/A	0.2	0.2	2.6	2.064	239.5	N/A
	7.5	10.5	0.5	32.9	1.1	1.6	2.1	21.5	2.328	4.0	N/A
	15	17	0.2	4.1	1.1	1.3	0.6	7.3	2.145	67.0	N/A
	20	22	0.3	2.9	1.0	1.3	1.6	12.3	2.192	19.8	N/A
	30	32	0.2	0.0	1.0	1.2	1.1	11.6	2.177	30.9	N/A
	40	42	N/A	N/A	N/A	N/A	N/A	N/A	N/A	N/A	N/A
	50	52	0.2	13.2	1.0	1.2	0.7	8.7	2.165	65.7	N/A

Date	Intended Depth (cm)	Actual Depth (cm)	NOx (µM)	NO_2^- (nM)	NH_4^+ (µM)	DIN (µM)	PO_4^{3-} (µM)	$Si(OH)_4$ (µM)	DIC (mM)	DO (µM)	Fe (µM)
12/15/08	0	0	0.2	9.0	1.0	1.2	0.3	1.5	N/A	249.6	N/A
	7.5	10.5	0.2	0.0	1.0	1.2	1.0	3.4	N/A	8.2	N/A
	15	18	0.2	5.5	1.7	1.9	0.8	8.9	N/A	0.0	N/A
	20	23	0.4	28.1	9.3	9.8	1.6	5.1	N/A	1.9	N/A
	30	33	0.4	8.0	9.4	9.8	1.5	11.0	N/A	0.7	N/A
	40	43	N/A	N/A	N/A	N/A	N/A	N/A	N/A	N/A	N/A
	50	53	0.2	14.6	0.9	1.1	0.9	9.4	N/A	1.0	N/A
6/1/09	0	0	0.3	0.0	0.9	1.2	0.2	3.8	N/A	N/A	N/A
	7.5	7.5	0.2	0.0	0.8	1.0	2.1	10.2	N/A	N/A	N/A
	15	15	0.4	0.0	0.8	1.2	2.8	9.7	N/A	N/A	N/A
	20	20	3.4	74.2	5.8	9.3	2.4	8.2	N/A	N/A	N/A
	30	30	1.5	39.0	0.8	2.3	2.3	6.4	N/A	N/A	N/A
	40	40	0.3	106.1	0.8	1.1	0.7	5.4	N/A	N/A	N/A
	50	50	5.7	88.2	2.7	8.4	0.3	9.1	N/A	N/A	N/A
12/2/09	0	0	0.0	27.2	0.4	0.4	0.3	0.1	2.130	N/A	0.5
	7.5	7.5	0.1	10.8	14.3	14.4	2.1	13.4	2.491	N/A	2.8
	15	15	0.2	16.1	14.6	14.8	3.9	12.3	2.367	N/A	2.4
	20	20	0.1	5.1	15.0	15.1	3.3	15.1	2.378	N/A	2.6
	30	30	0.2	14.7	7.6	7.7	3.4	12.1	2.317	N/A	0.9
	40	40	5.3	7.4	0.0	5.3	1.6	7.6	2.248	N/A	0.5
	50	50	4.0	274.1	0.0	4.0	1.3	8.7	2.267	N/A	0.5
12/18/09	0	0	0.2	0.0	0.0	0.2	0.3	0.0	2.143	N/A	N/A
	7.5	7.5	0.2	22.8	5.6	5.8	2.0	14.2	2.369	N/A	N/A
	15	15	0.7	21.4	7.6	8.3	3.3	13.1	2.350	N/A	N/A
	20	20	1.2	42.3	5.0	6.2	2.7	13.0	2.305	N/A	N/A
	30	30	1.6	197.7	2.1	3.7	3.0	10.0	2.270	N/A	N/A
	40	40	N/A	N/A	N/A	N/A	N/A	N/A	N/A	N/A	N/A
	50	50	2.7	239.4	0.0	2.7	1.0	8.3	2.208	N/A	N/A

Date	Intended Depth (cm)	Actual Depth (cm)	NOx (µM)	NO_2^- (nM)	NH_4^+ (µM)	DIN (µM)	PO_4^{3-} (µM)	$Si(OH)_4$ (µM)	DIC (mM)	DO (µM)	Fe (µM)
1/29/10	0	0	0.1	10.7	0.0	0.1	0.5	2.9	2.162	N/A	N/A
	7.5	7.5	0.4	29.5	6.3	6.7	2.0	13.2	2.297	N/A	N/A
	15	15	2.4	39.1	2.1	4.6	2.9	10.7	2.269	N/A	N/A
	20	20	2.5	47.1	1.5	4.1	2.9	11.1	2.263	N/A	N/A
	30	30	4.9	52.2	0.8	5.7	2.7	10.7	2.261	N/A	N/A
	40	40	9.7	10.2	0.8	10.4	1.3	7.9	2.151	N/A	N/A
	50	50	6.2	24.8	0.8	6.9	1.1	7.1	2.150	N/A	N/A

Appendix B

For the oxygen contamination experiment "Delta Time" is the time from which the sample was collected and it was analyzed for DO (see Methods Section). "Old" versus "New" syringe experiment was designed to observe any breakdown of the syringes over time to insure no additional oxygen contamination. "Old" syringe was a syringe used many times in the field while the "new" syringe was tested directly from the package.

Delta Time	DO (% Sat)	DO (mg/L)	DO (µM)
1	0.9	0.07	2.19
10	8.7	0.62	19.38
17	9.1	0.67	20.94
23	10.4	0.75	23.44
30	12.6	0.91	28.44
31	11.9	0.86	26.88
41	11.5	0.84	26.25
"Old" and "New" syringes Experiment			
10	8.8	0.64	"Old" Syringe
10	8.7	0.62	"New" Syringe

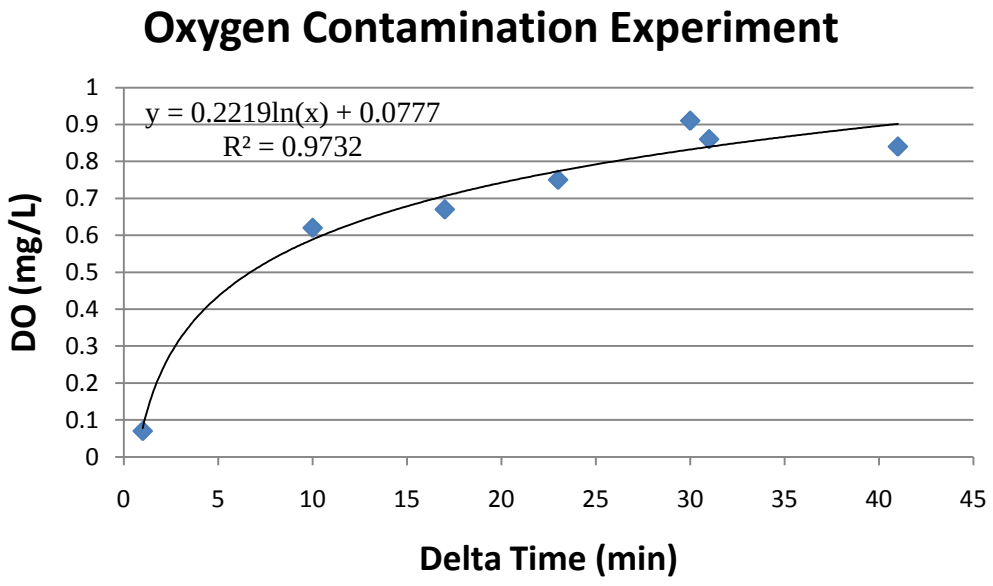

Appendix C

Nitrate in porewater samples collected 18 December 2009 and 29 January 2010 was reduced using a Cadmium column or nitrate reductase enzyme (see Methods Section) to compare NO_3 methods. Once reduced to NO_2, samples were analyzed for total nitrate + nitrite using the standard colormetric method (Grasshoff et al., 1983).

With Cadmium							
12/18/2009	Absorbance			1/29/2010	Absorbance		
	Run 1	Run 2	Run 3		Run 1	Run 2	Run 3
0	0.01	0.01	0.02	0	0.01	0.01	0.01
7.5	0.01	0.01	0.01	7.5	0.02	0.02	0.02
15	0.02	0.03	0.03	15	0.10	0.10	0.08
20	0.04	0.04	0.03	20	0.09	0.10	0.08
30	0.05	0.07	0.03	30	0.21	0.21	0.17
40	N/A	N/A	N/A	40	0.32	0.35	0.23
50	0.10	0.12	0.13	50	0.25	0.28	0.21
12/18/2009	Concentration (µM)			1/29/2010	Concentration (µM)		
	Run 1	Run 2	Run 3		Run 1	Run 2	Run 3
0	-0.23	-0.20	0.04	0	-0.08	-0.14	-0.14
7.5	-0.11	-0.11	-0.02	7.5	0.10	0.13	0.10
15	0.24	0.42	0.39	15	2.49	2.46	1.96
20	0.66	0.72	0.57	20	2.22	2.43	2.01
30	1.13	1.54	0.54	30	5.76	5.82	4.61
40	N/A	N/A	N/A	40	8.89	9.83	6.32
50	2.66	3.19	3.37	50	7.06	7.80	5.91

With Enzyme							
12/18/2009	Absorbance			1/29/2010	Absorbance		
	Run 1	Run 2	Run 3		Run 1	Run 2	Run 3
0	0.03	0.03	0.03	0	0.03	0.03	0.03
7.5	0.03	0.03	0.03	7.5	NaN	0.03	0.03
15	0.05	0.03	0.03	15	0.05	0.05	0.05
20	0.03	0.04	0.03	20	0.05	0.05	0.06
30	0.04	0.04	0.04	30	0.08	0.08	0.08
40	N/A	N/A	N/A	40	0.12	0.12	0.11
50	0.06	0.06	0.06	50	0.10	0.10	0.09
12/18/2009	NO_3 Concentration (µM)			1/29/2010	NO_3 Concentration (µM)		
	Run 1	Run 2	Run 3		Run 1	Run 2	Run 3
0	0.09	0.19	0.09	0	0.60	0.49	0.49
7.5	0.19	0.19	0.49	7.5	0.70	0.90	0.60
15	0.8	0.70	0.70	15	2.62	2.72	2.62
20	0.80	1.00	0.90	20	2.72	2.62	3.32
30	1.81	1.71	1.81	30	5.65	5.34	5.14
40	N/A	N/A	N/A	40	9.69	9.69	8.58
50	3.32	3.22	3.22	50	7.77	7.67	6.35

Appendix D

Tidal height from ADCP, significant wave heights from ADCP and nearbed velocities from ADCP for June to December 2008 at Kilo Nalu 12 m site.

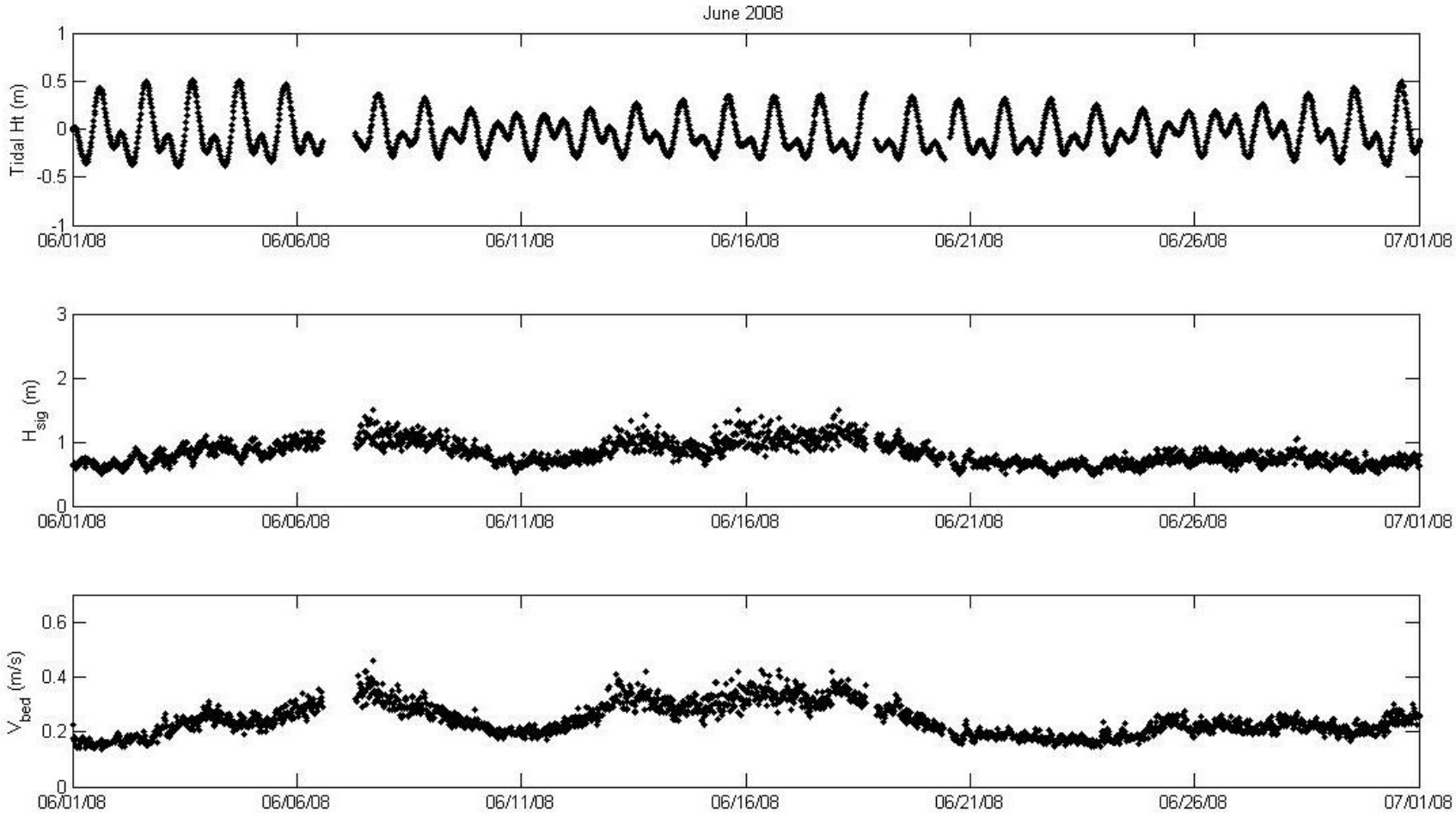
June 2008
Tidal Ht (m)
1
0.5
0
-0.5
-1
06/01/08
06/06/08
06/11/08
06/16/08
06/21/08
06/26/08
07/01/08
H_{sig} (m)
3
2
1
0
V_{bed} (m/s)
0.6
0.4
0.2
0

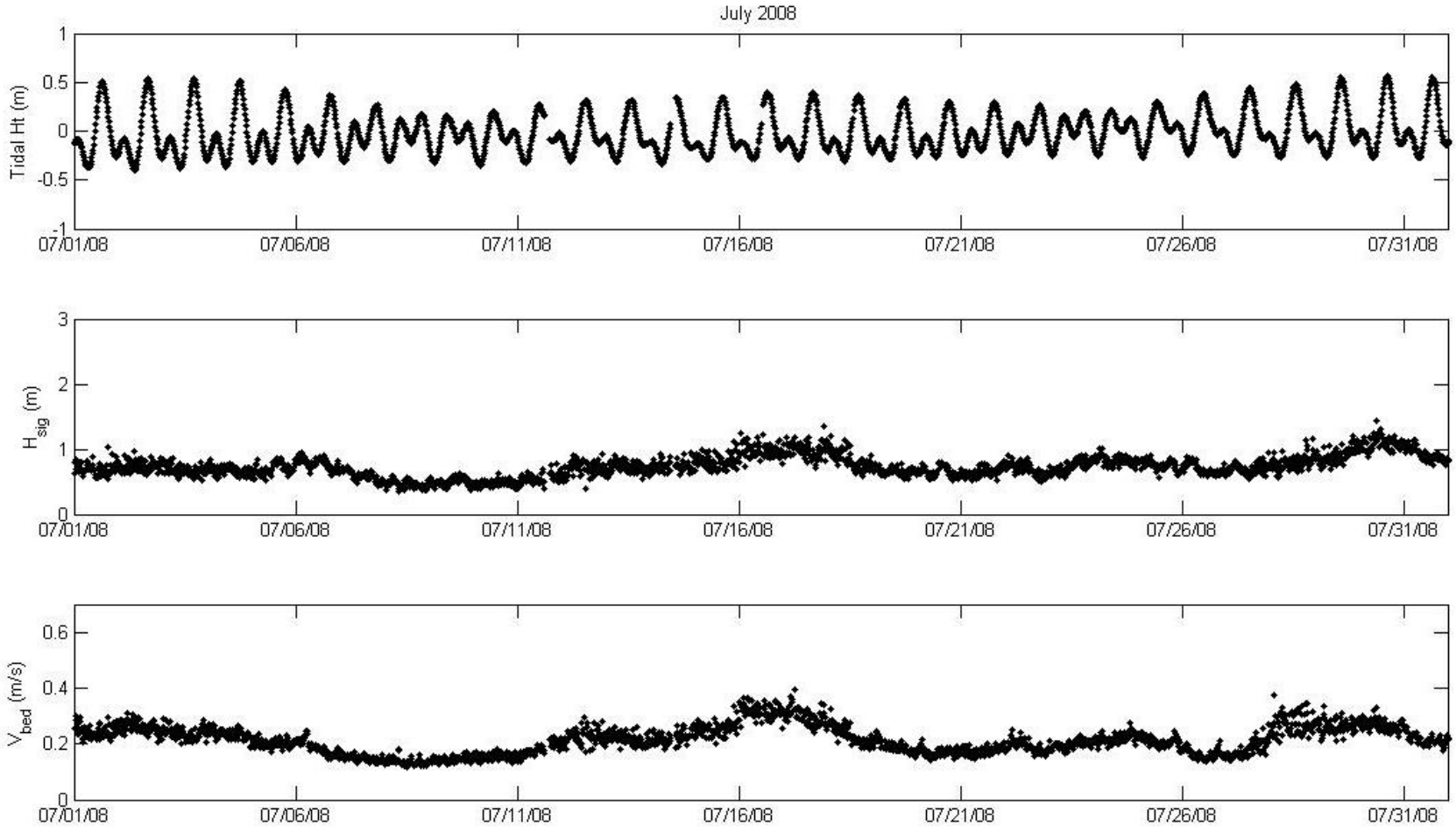
July 2008
Tidal Ht (m)
1
0.5
0
-0.5
-1
07/01/08
07/06/08
07/11/08
07/16/08
07/21/08
07/26/08
07/31/08
H_sig (m)
3
2
1
0
V_bed (m/s)
0.6
0.4
0.2
0

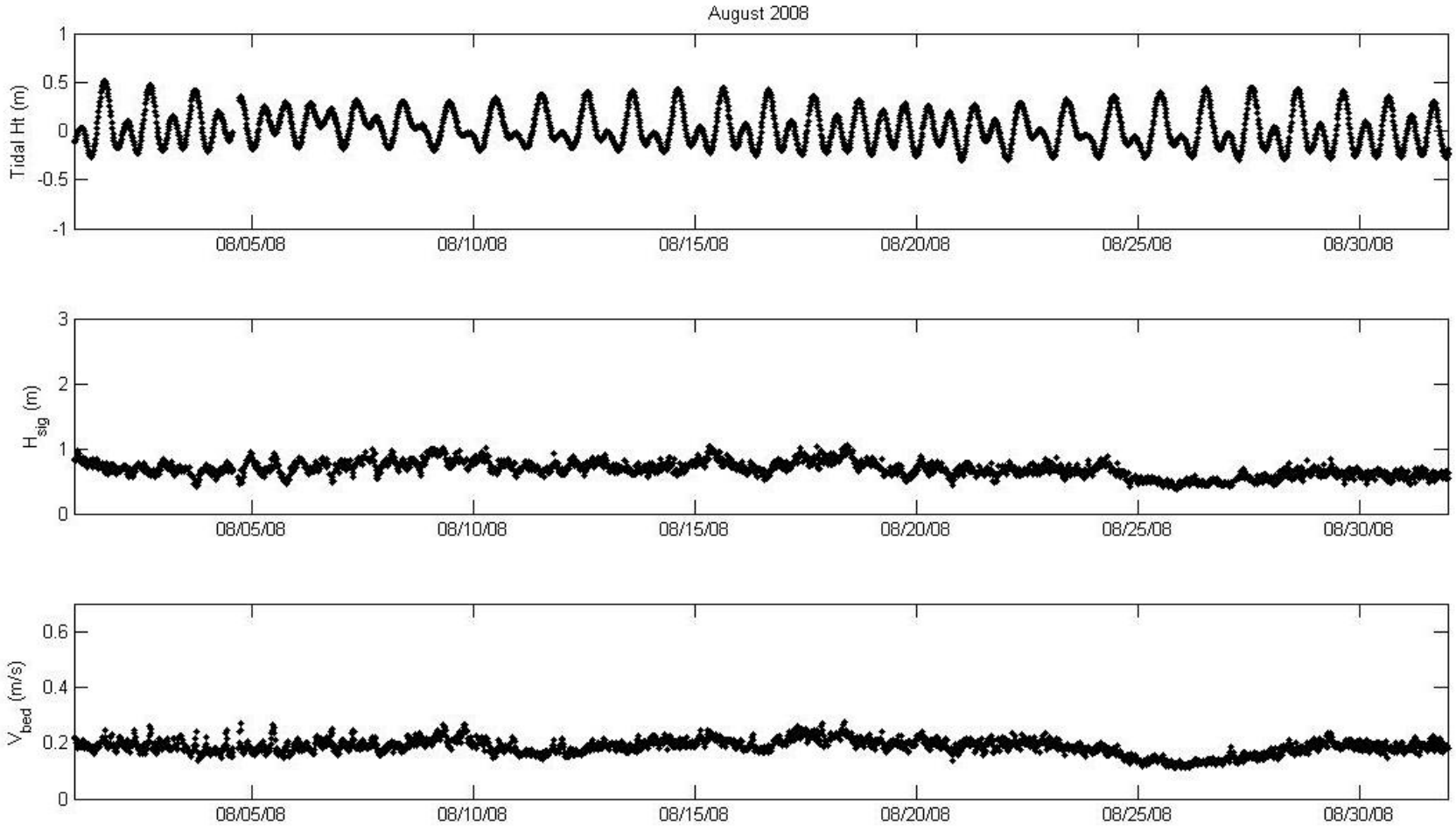
August 2008
Tidal Ht (m)
1
0.5
0
-0.5
-1
08/05/08
08/10/08
08/15/08
08/20/08
08/25/08
08/30/08
H_{sig} (m)
3
2
1
0
V_{bed} (m/s)
0.6
0.4
0.2
0

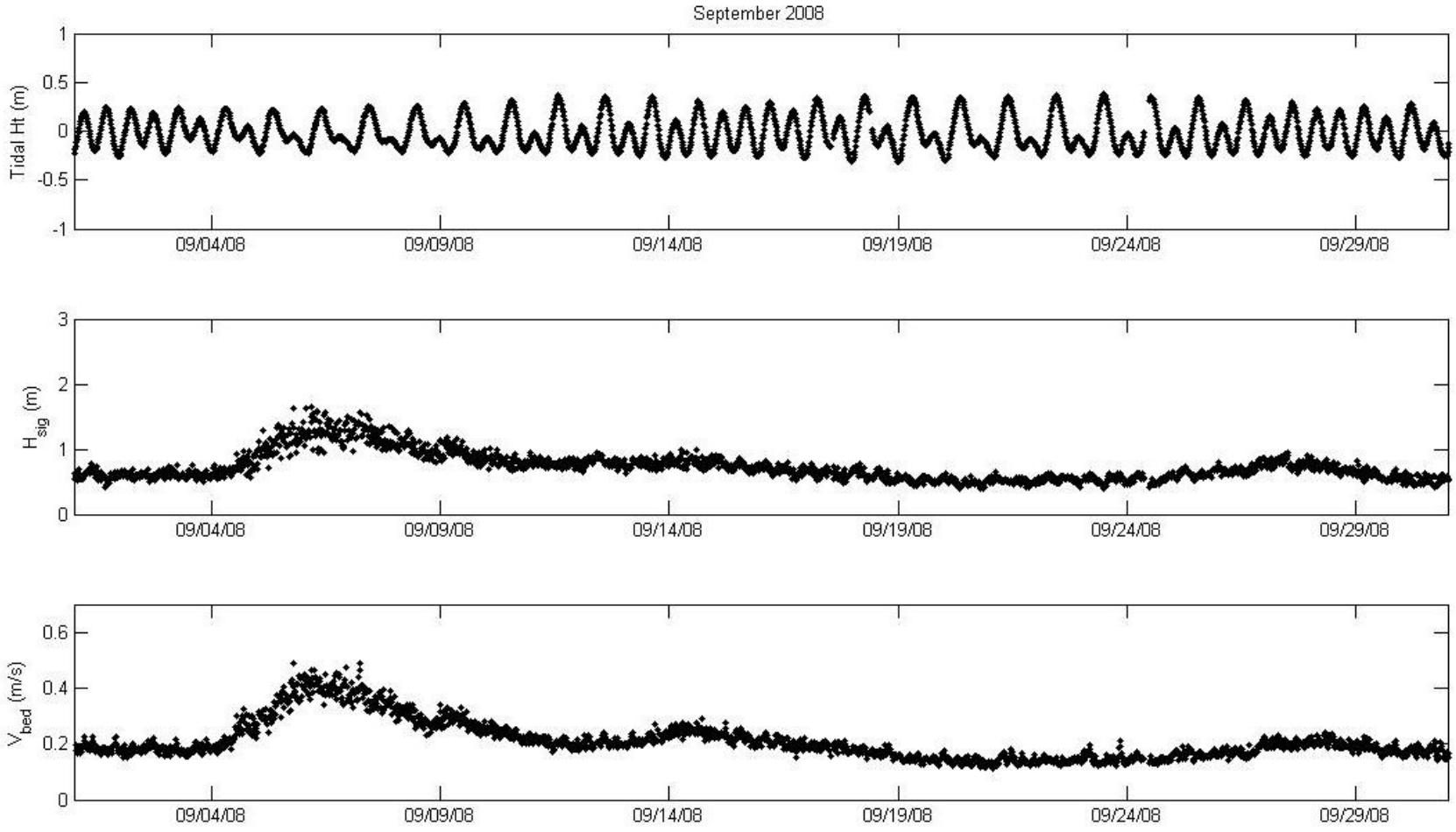
September 2008
Tidal Ht (m)
1
0.5
0
-0.5
-1
09/04/08
09/09/08
09/14/08
09/19/08
09/24/08
09/29/08
H_sig (m)
3
2
1
0
V_bed (m/s)
0.6
0.4
0.2
0

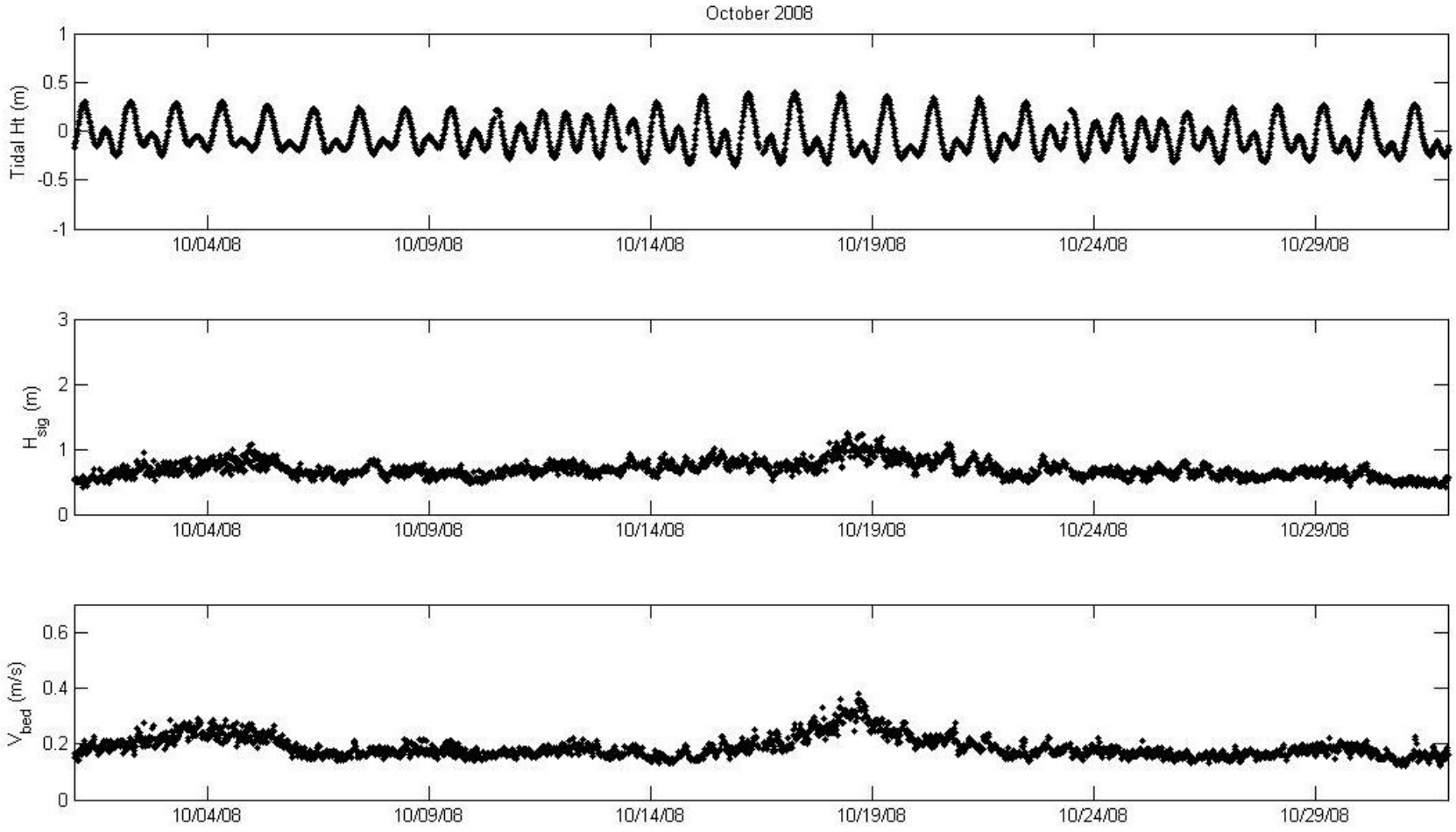
October 2008
Tidal Ht (m)
1
0.5
0
-0.5
-1
10/04/08
10/09/08
10/14/08
10/19/08
10/24/08
10/29/08
H_sig (m)
3
2
1
0
V_bed (m/s)
0.6
0.4
0.2
0

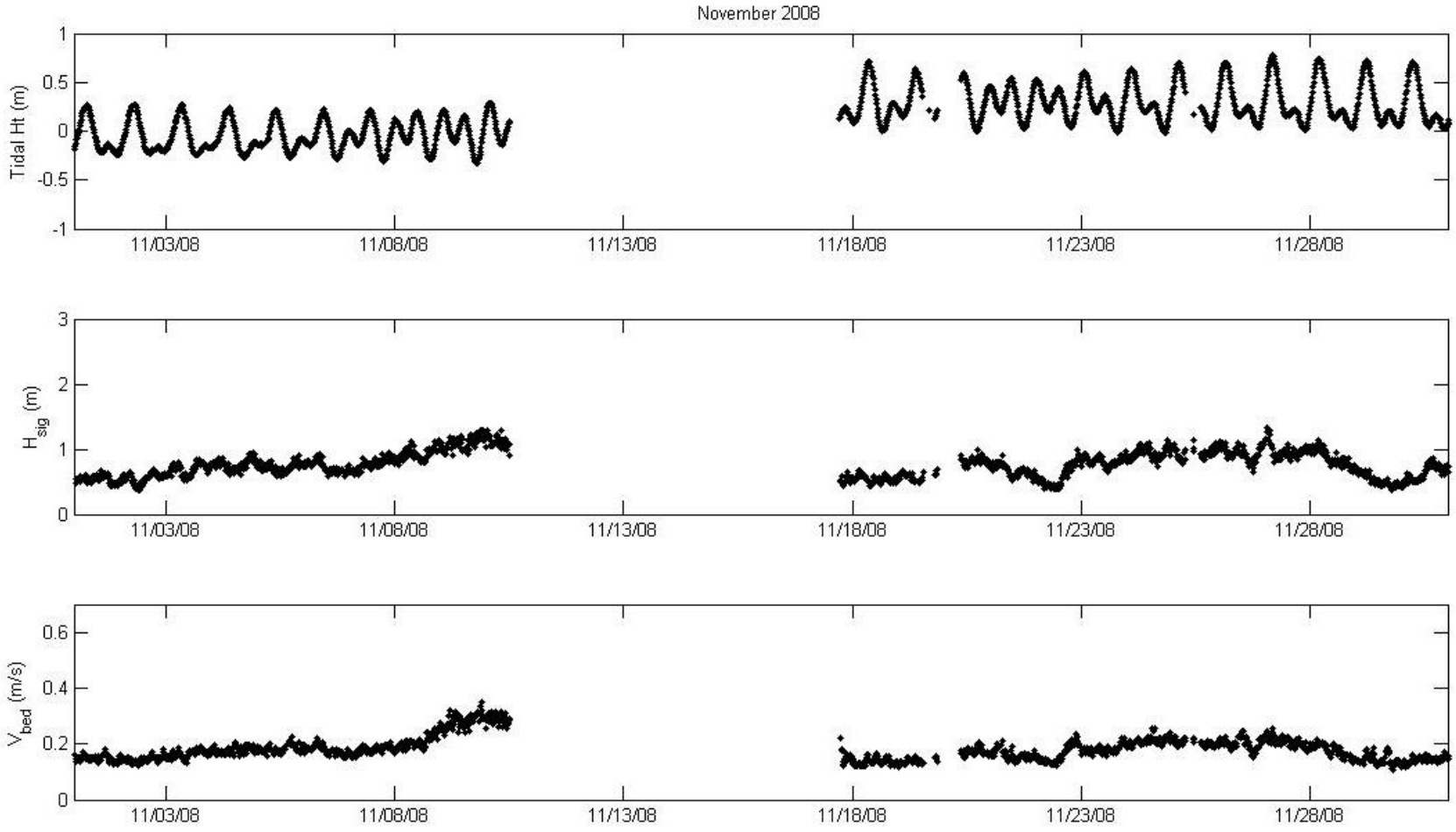
November 2008
Tidal Ht (m)
1
0.5
0
-0.5
-1
11/03/08
11/08/08
11/13/08
11/18/08
11/23/08
11/28/08
H_sig (m)
3
2
1
0
V_bed (m/s)
0.6
0.4
0.2
0

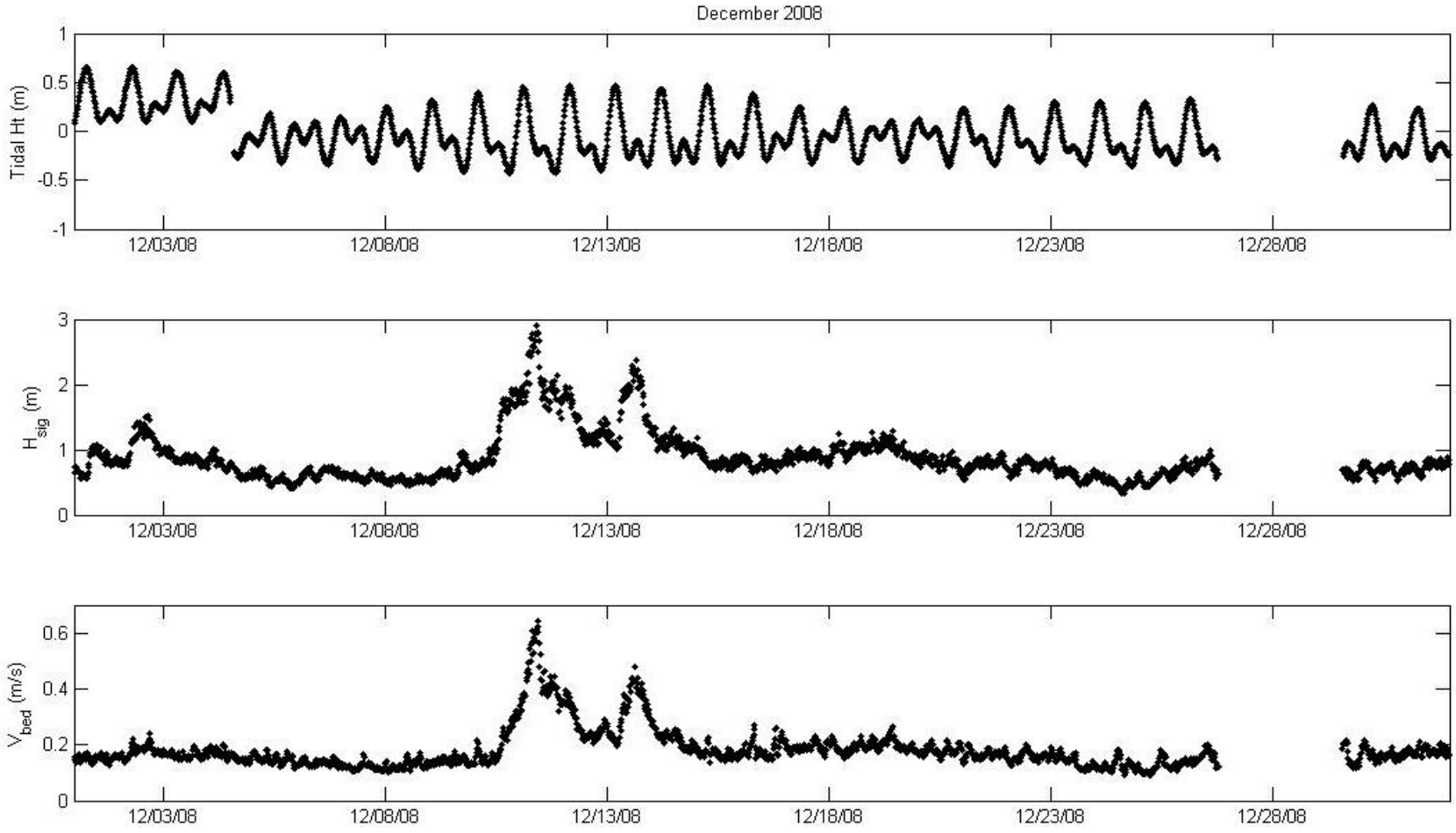
December 2008
Tidal Ht (m)
1
0.5
0
-0.5
-1
12/03/08
12/08/08
12/13/08
12/18/08
12/23/08
12/28/08
H_{sig} (m)
3
2
1
0
V_{bed} (m/s)
0.6
0.4
0.2
0

Appendix E

Bottom-water salinity from Seabird-37 CTD, bottom-water temperature from Seabird-37 CTD, bottom-water turbidity from ECO FLNTU and bottom-water fluorescence from ECO FLNTU for June to December 2008 for Kilo Nalu. ECO FLNTU fluorescence data has been corrected for biofouling (see Methods Section)

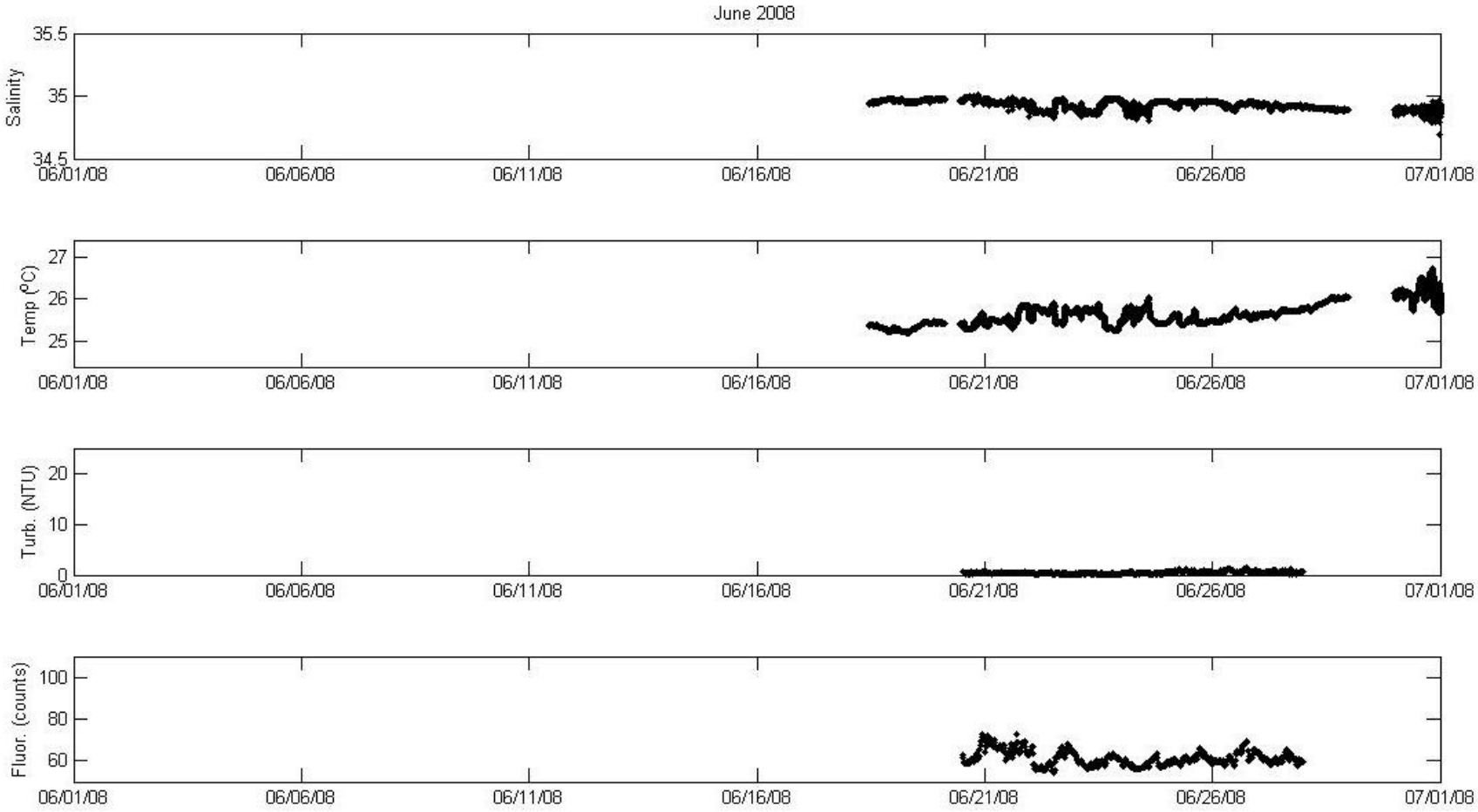
June 2008
Salinity
35.5
35
34.5
Temp (°C)
27
26
25
Turb. (NTU)
20
10
0
Fluor. (counts)
100
80
60
06/01/08
06/06/08
06/11/08
06/16/08
06/21/08
06/26/08
07/01/08

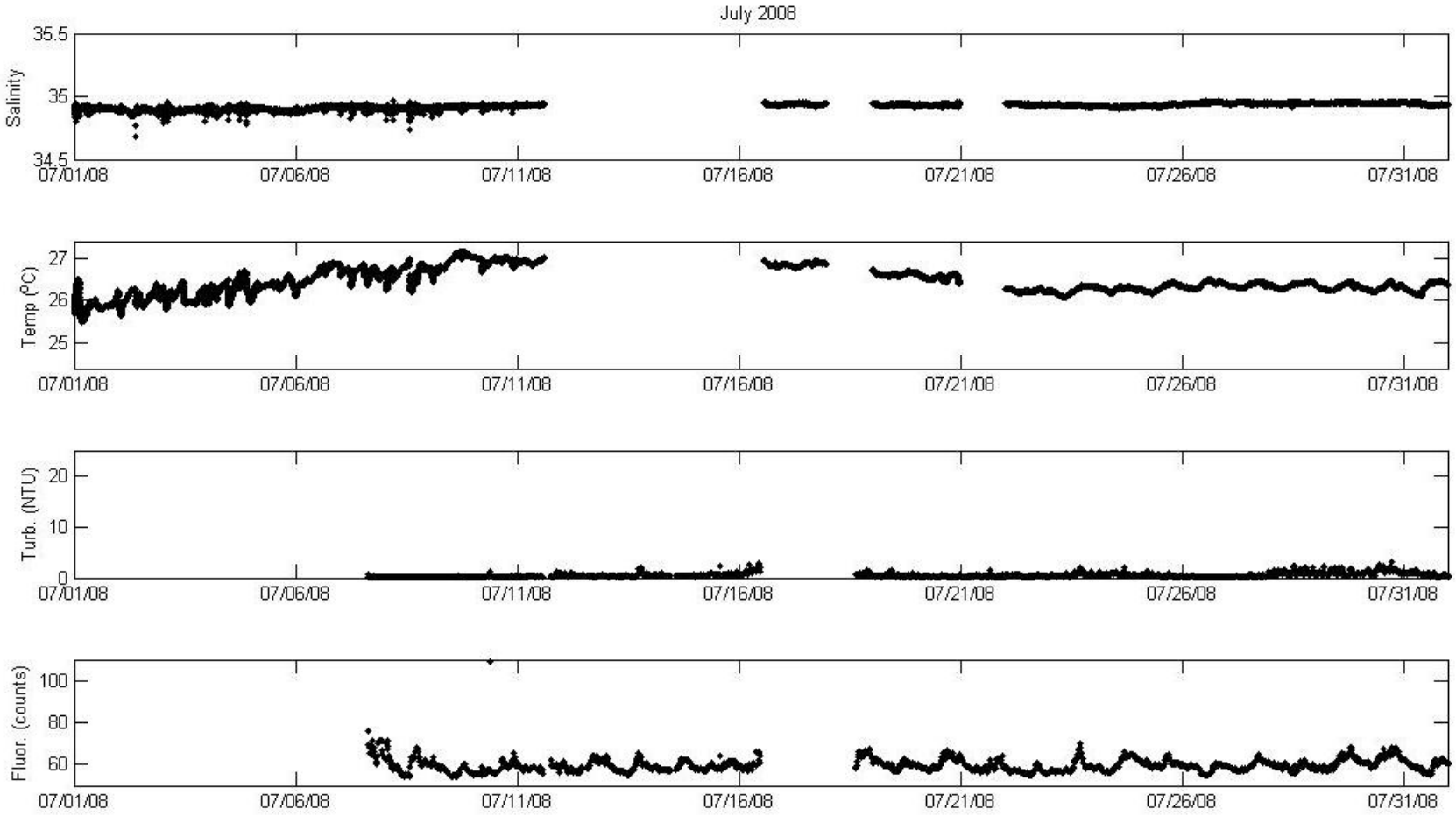
July 2008
Salinity
35.5
35
34.5
Temp (°C)
27
26
25
Turb. (NTU)
20
10
0
Fluor. (counts)
100
80
60
07/01/08
07/06/08
07/11/08
07/16/08
07/21/08
07/26/08
07/31/08

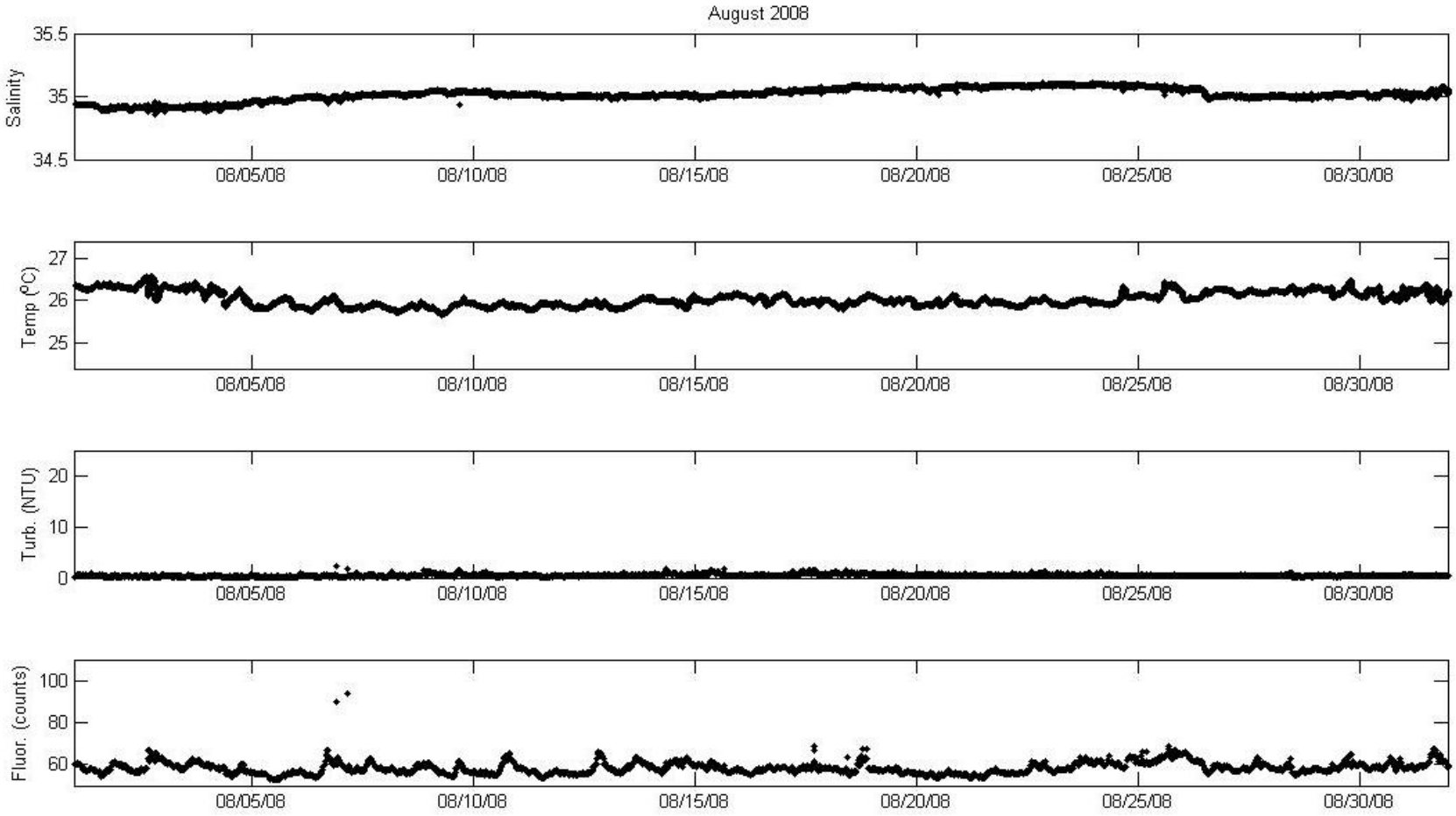
August 2008
Salinity
35.5
35
34.5
Temp (°C)
27
26
25
Turb. (NTU)
20
10
0
Fluor. (counts)
100
80
60
08/05/08
08/10/08
08/15/08
08/20/08
08/25/08
08/30/08

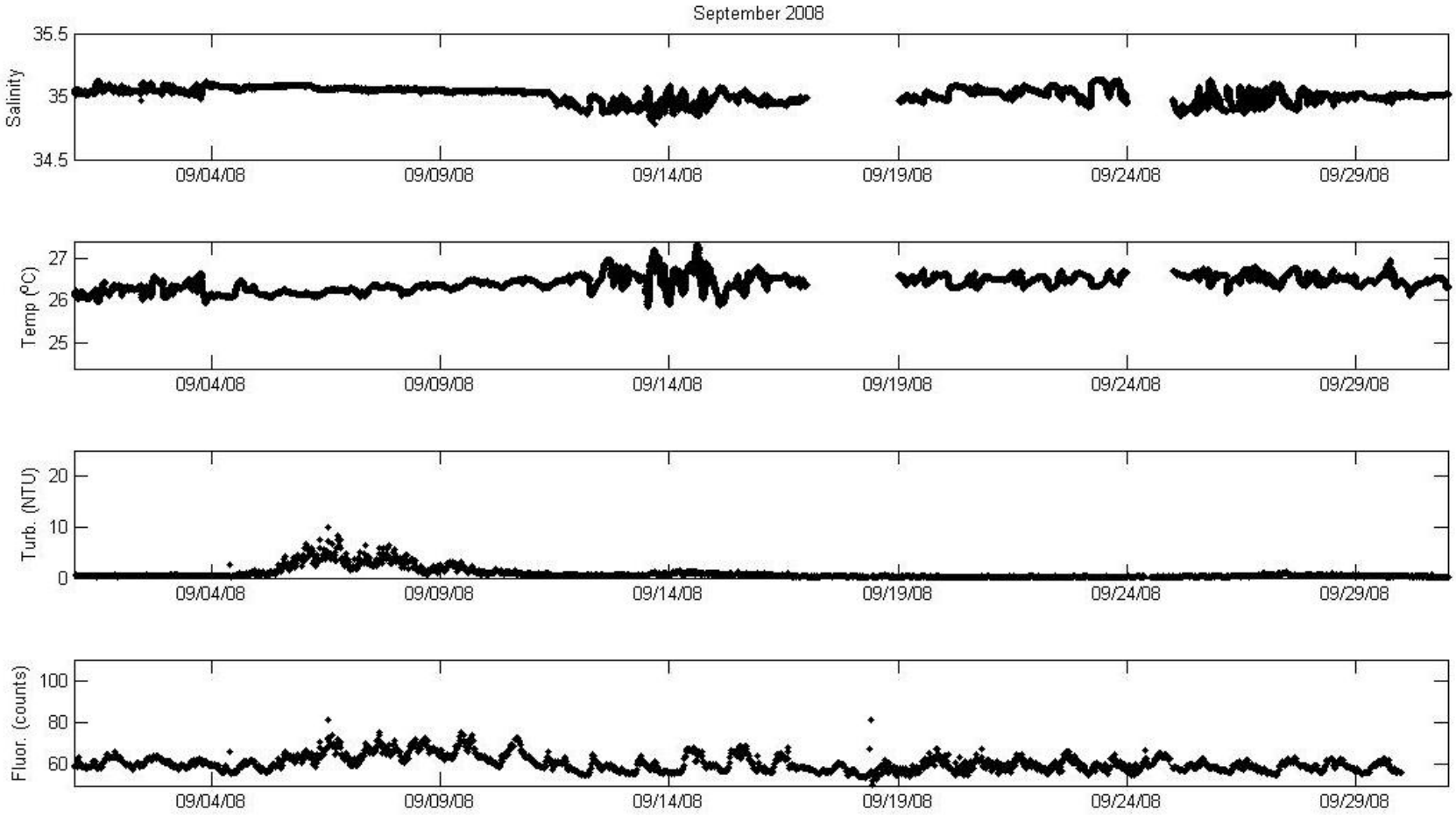
September 2008
Salinity
35.5
35
34.5
Temp (°C)
27
26
25
Turb. (NTU)
20
10
0
Fluor. (counts)
100
80
60
09/04/08
09/09/08
09/14/08
09/19/08
09/24/08
09/29/08

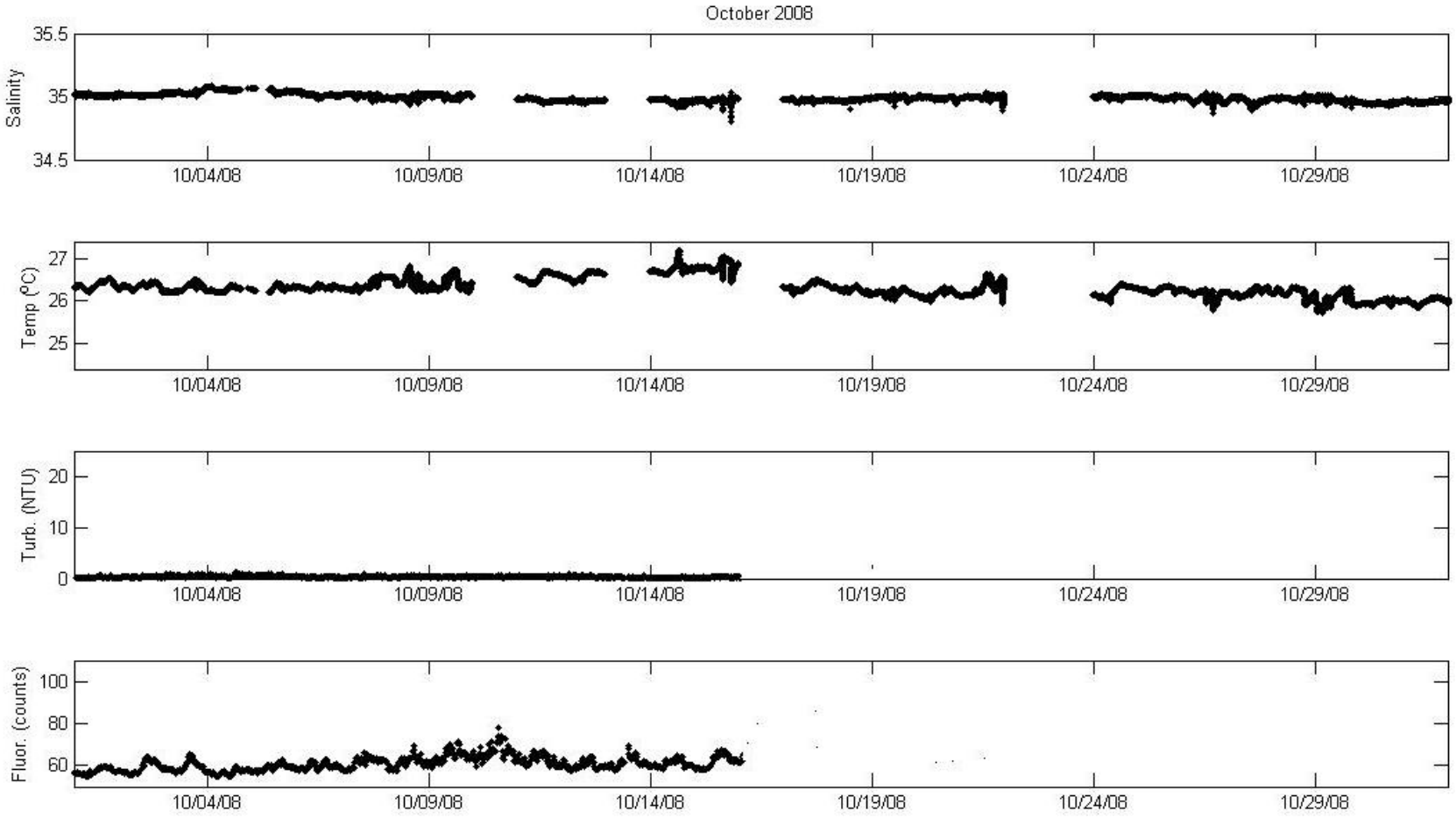
October 2008
Salinity
35.5
35
34.5
Temp (°C)
27
26
25
Turb. (NTU)
20
10
0
Fluor. (counts)
100
80
60
10/04/08
10/09/08
10/14/08
10/19/08
10/24/08
10/29/08

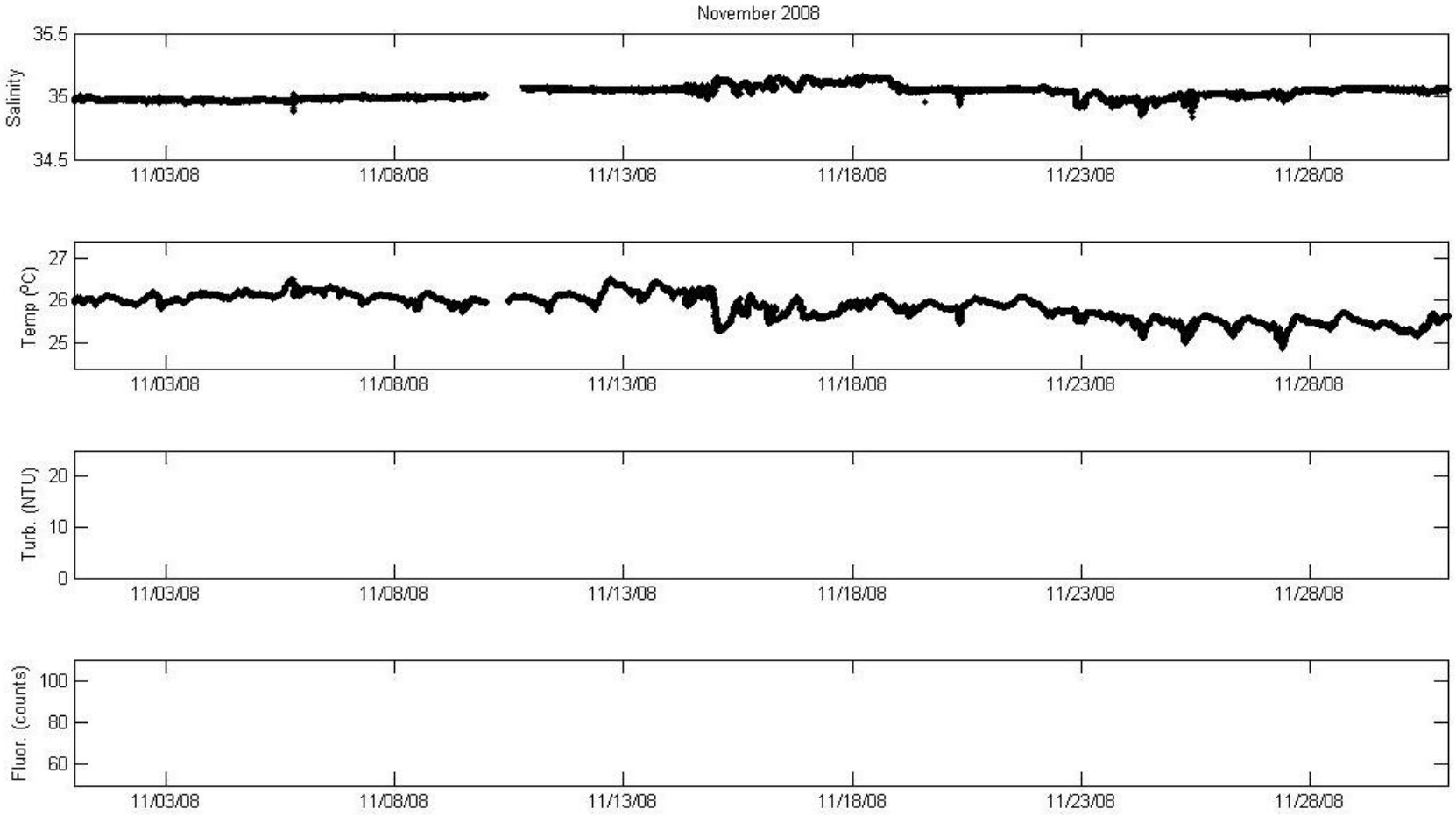
November 2008
Salinity
35.5
35
34.5
Temp (°C)
27
26
25
Turb. (NTU)
20
10
0
Fluor. (counts)
100
80
60
11/03/08
11/08/08
11/13/08
11/18/08
11/23/08
11/28/08

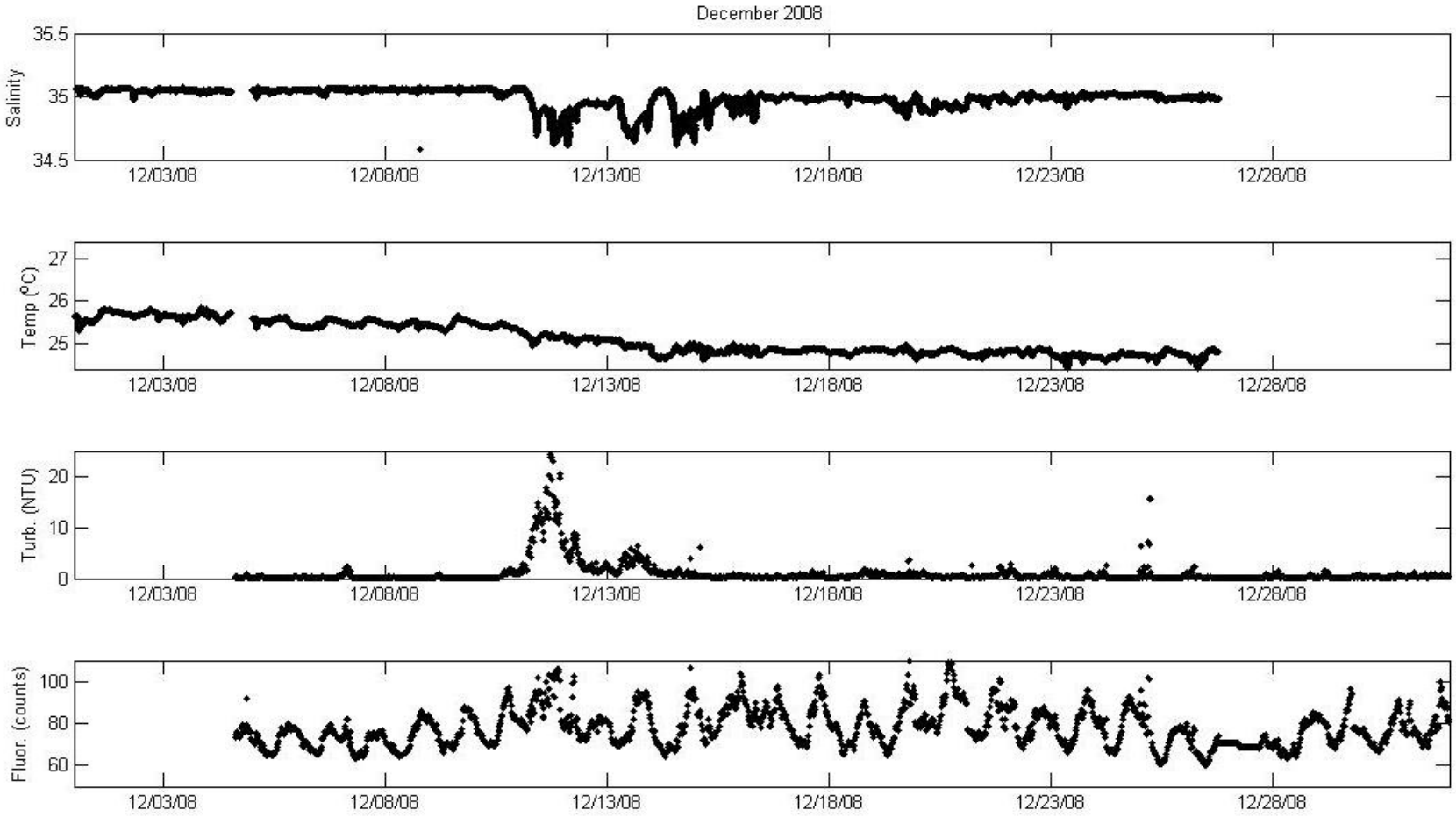
December 2008
Salinity
35.5
35
34.5
Temp (°C)
27
26
25
Turb. (NTU)
20
10
0
Fluor. (counts)
100
80
60
12/03/08
12/08/08
12/13/08
12/18/08
12/23/08
12/28/08